AD_____

AWARD NUMBER: W81XWH-09-1-0220

TITLE: 'Novel gene C17orf37 in Prostate Cancer Progression and Metastasis: A Prospective Biomarker'

PRINCIPAL INVESTIGATOR: Subhamoy Dasgupta

CONTRACTING ORGANIZATION: University of North Texas Health Science Center
Fort Worth, Texas 76107

REPORT DATE: May 2010

TYPE OF REPORT: Annual Summary

PREPARED FOR: U.S. Army Medical Research and Materiel Command
Fort Detrick, Maryland 21702-5012

REPORT DOCUMENTATION PAGE

Form Approved
OMB No. 0704-0188

1. REPORT DATE *(DD-MM-YYYY)*	2. REPORT TYPE	3. DATES COVERED *(From - To)*
01-05-2010	Annual Summary	1 May 2009 - 30 April 2010

4. TITLE AND SUBTITLE
'Novel gene C17orf37 in Prostate Cancer Progression and Metastasis:

A Prospective Biomarker'

5a. CONTRACT NUMBER

5b. GRANT NUMBER
W81XWH-09-1-0220

5c. PROGRAM ELEMENT NUMBER

6. AUTHOR(S)
Subhamoy Dasgupta E-mail: sdasgupt@live.unthsc.edu

Jamboor Vishwanatha. Ph.D. E-mail: jvishwan@hsc.unt.edu

5d. PROJECT NUMBER

5e. TASK NUMBER

5f. WORK UNIT NUMBER

7. PERFORMING ORGANIZATION NAME(S) AND ADDRESS(ES)

University of North Texas Health Science Center
Fort Worth, Texas 76107

8. PERFORMING ORGANIZATION REPORT NUMBER

9. SPONSORING / MONITORING AGENCY NAME(S) AND ADDRESS(ES)
U.S. Army Medical Research and Materiel Command
Fort Detrick, MD 21702

10. SPONSOR/MONITOR'S ACRONYM(S)

11. SPONSOR/MONITOR'S REPORT NUMBER(S)

12. DISTRIBUTION / AVAILABILITY STATEMENT
Approved for public release; distribution unlimited

13. SUPPLEMENTARY NOTES

14. ABSTRACT
The project focuses on novel gene named *Chromosome 17 open reading frame 37 (C17orf37)* in prostate cancer progression and metastasis. Although the gene is overexpressed in different forms of cancer, its expression and role in prostate cancer is poorly understood. The Aims of the project are to (1) To establish the correlation of C17orf37 protein expression with poor pathological and prognostic variables in prostatic adenocarcinomas, and (2) To directly demonstrate the biological consequences of C17orf37 overexpression in promoting prostate tumor metastasis and elucidate the molecular mechanisms regulating the process *in vivo*. This is the first annual report, and we have identified that C17orf37 is overexpressed in prostate cancer patients compared to normal prostatic tissues. We also discovered that overexpression of C17orf37 potentiates migration and invasion of prostate cancer cells through Akt/NF-κB downstream target genes. We have also established the stable cell lines expressing C17orf37, and currently evaluating role of C17orf37 in prostate cancer metastasis.

15. SUBJECT TERMS

16. SECURITY CLASSIFICATION OF:			17. LIMITATION OF ABSTRACT	18. NUMBER OF PAGES	19a. NAME OF RESPONSIBLE PERSON
a. REPORT	b. ABSTRACT	c. THIS PAGE			19b. TELEPHONE NUMBER *(include area code)*
U	U	U	UU	47	

Table of Contents

INTRODUCTION

This project focuses on a novel gene named C17orf37 located in the 17q12 amplicon of human chromosome. The 17q12 amplicon contains numerous genes that have been shown to play important role in prostate cancer progression and metastasis *(1-4)*. C17orf37 has been found to be highly expressed in human cancers; however its expression profile in prostate cancer and functional significance in cancer biology is unknown. We recently identified that C17orf37 promotes migration and invasion of prostate cancer cells. The objective of the current project is to characterize the functional importance of C17orf37 overexpression in prostate cancer progression and elucidate the molecular pathways that contribute to the development of invasive and metastatic cancer. Successful completion of the project will allow us to understand the role of the novel gene C17orf37 in cancer cells and validate it as a potential target for cancer therapy.

BODY

Task 1. *To establish the correlation of C17orf37 protein expression with poor pathological and prognostic variables in prostatic adenocarcinomas.*

Findings:

We evaluated the expression of C17orf37 in normal prostate, benign prostatic hyperplasia (BPH), moderately differentiated, and poorly differentiated prostate adenocarcinoma clinical samples. Our data suggests that C17orf37 expression is basal in normal and BPH specimens, however its expression is increased in advanced stages of the disease. In moderately differentiated specimens, C17orf37 expression was found to be intense in the neoplastic glands and stromal cells surrounding the prostatic glands. Strong C17orf37 expression was found throughout the poorly differentiated prostate cancer sections with intense diffused stain in the stroma around the malignant cell mass and invasive edges. C17orf37 expression was intense in the fused prostatic glands of poorly differentiated prostatic cancer. Surprisingly, we identified intense C17orf37 staining in prostatic intraepithelial neoplasm (PIN), which suggests that C17orf37 is expressed in the early lesions of prostate cancer (Figure 1). These studies resulted in the publication of an original research article *(5)*.

Ongoing experiments: Currently we are correlating the expression of C17orf37 with other prognostic variables of prostate adenocarcinoma including hormonal dependency, disease recurrence, and metastasis.

Task 2. *To directly demonstrate the biological consequences of C17orf37 overexpression in promoting prostate tumor metastasis and elucidate the molecular mechanisms regulating the process in vivo.*

Finding 1: Stable overexpression of C17orf37 increases the migratory and invasive potential of prostate cancer cells.

For generation of stable cells, DU-145 cells were transfected using Lipofectamine 2000, with either GFP (empty-vector) or GFP-C17orf37 plasmid DNA for 24hours. Stable transfected cell populations were challenged in complete medium supplemented with 500µg/ml G418 (Invitrogen, Carlsbad, CA) for about 2 weeks. Stable cells were maintained as polyclonal populations obtained from DU-145 cells transfected with GFP vector (DU-GFP) and DU-145 cells transfected with GFP-C17orf37 plasmid (DU-GFP-C17orf37-1 and 2). Stable overexpression of GFP-C17orf37 construct in DU-145 cells (DU-GFP-C17orf37) dramatically increased the invasiveness ~2.0-2.5 fold compared to parental DU-145 cells (Figure 2) in Matrigel Invasion Assay, indicating overexpression of C17orf37 protein leads to increased invasive behavior in prostate cancer cells. These studies resulted in the publication of an original research article *(5)*.

Finding 2.

To investigate whether C17orf37 protein has any effect on the metastasis related genes, we analyzed the expression of several genes that facilitate prostate cancer metastasis and promote ECM cleavage. We found that overexpression of C17orf37 increases endogenous MMP-9, uPA and VEGF expression compared to vector treated cells. *MMP-9, uPA* and *VEGF* genes are transcriptionally up-regulated by NF-κB *(6)*. We performed

EMSA to evaluate the DNA binding activity of NF-κB in C17orf37 overexpressed cells. Overexpression of C17orf37 increases the DNA binding activity of NF-κB, suggesting C17orf37 increases migration and invasion in prostate cancer by NF-κB mediated genes MMP-9, uPA and VEGF. In prostate cancer cells, constitutive activation of NF-κB is mediated by upstream protein kinase B (PKB/Akt)*(7)*, we performed western immunoblot to detect the levels of phosphorylated Akt (p-Akt) and total Akt. p-Akt is the active form of the protein that cascades the intracellular signaling and we observed phosphorylation of Akt was significantly higher in the stable clones compared to vector control cells (DU-GFP) (Figure 3). These results demonstrate that C17orf37 mediates prostate cancer cell migration and invasion through NF-κB downstream target genes MMP-9, UPA and VEGF. These results were reported in an original article.

Ongoing experiments: Currently we are performing *in vivo* xenograft studies in athymic mice to understand the role of C17orf37 in prostate cancer migration and invasion.

KEY RESEARCH ACCOMPLISHMENTS

- C17orf37 is overexpressed in prostate cancer patients, and the expression of the protein is increased in the advanced stage of the disease.
- Overexpression of C17orf37 in prostate cancer cells promotes migration and invasion.
- C17orf37 modulates Akt phosphorylation and thereby activates NF-κB DNA binding activity, thereby upregulates downstream target genes MMP-9, uPA and VEGF.
- We propose a model which suggests, C17orf37 may act as a membrane bound adapter molecule triggering downstream signaling through Akt/NF-κB pathway *(8)*.

REPORTABLE OUTCOMES

To date, 2 articles have been published and 1 abstract has been presented as a result of funding from this grant:

Articles:

1. **Dasgupta S**, Wasson LM, Rauniyar N, Prokai L, Borejdo J, Vishwanatha JK. (2009). Novel gene C17orf37 in 17q12 amplicon promotes migration and invasion of prostate cancer cells. *Oncogene* **28:**2860-2872.

2**. Dasgupta S** and Vishwanatha JK. C17orf37 Molecule Page. *UCSD-Nature Molecule Pages*.(2009) doi:10.1038/mp.a004151.01

Presentations:

Dasgupta, S and Vishwanatha JK. Importance of C17orf37 prenyl modification in cancer cell migration and invasion. *Cancer Res* 2009;69(23 Suppl):A9

[Presented at the First AACR Conference on Frontiers in Basic Cancer Research, at Boston, MA on October 2009]

CONCLUSIONS

Our study has advanced our understanding about the biological role of C17orf37. Our study demonstrates that C17orf37 is overexpressed in prostate cancer patients compared to normal tissues. Overexpression of C17orf37 contributes to the development of invasive prostate cancer through NF-κB downstream target genes. We find that C17orf37 modulates Akt activity as a membrane bound adapter molecule. Interestingly, we identified C17orf37 has a prenylation motif at the C-terminal carboxyl end. Prenylated proteins are modified by addition of isoprenyl groups at the 'Caax' motif by prenyl transferase enzymes. In addition to our proposed experiments, we are also evaluating the importance of C17orf37 prenyl-modification in prostate cancer invasion and metastasis. We believe our results are the first report *(5)* to deduce the functional importance of so-called 'hypothetical protein' C17orf37 that may be considered as a potential therapeutic target for cancer therapy.

REFERENCES

1. P. Kauraniemi, A. Kallioniemi, *Endocr Relat Cancer* **13**, 39 (2006).

2. P. Kauraniemi, T. Kuukasjärvi, G. Sauter, A. Kallioniemi, *Am J Pathol* **163**, 1979 (2003).

3. E. E. Evans *et al.*, *Mol Cancer Ther* **5**, 2919 (2006).

4. N. Maqani *et al.*, *Mol. Cancer. Res.* **4**, 449 (2006).

5. S. Dasgupta *et al.*, *Oncogene* **28**, 2860 (2009).

6. J. Suh, A. B. Rabson, *J. Cell. Biochem.* **91**, 100 (2004).

7. J. A. Fresno Vara *et al.*, *Cancer Treat. Rev.* **30**, 193 (2004).

8. S. Dasgupta, J. K. Vishwanatha, *UCSD-Nature Molecule Pages* (2009).

Appendices

Figure 1

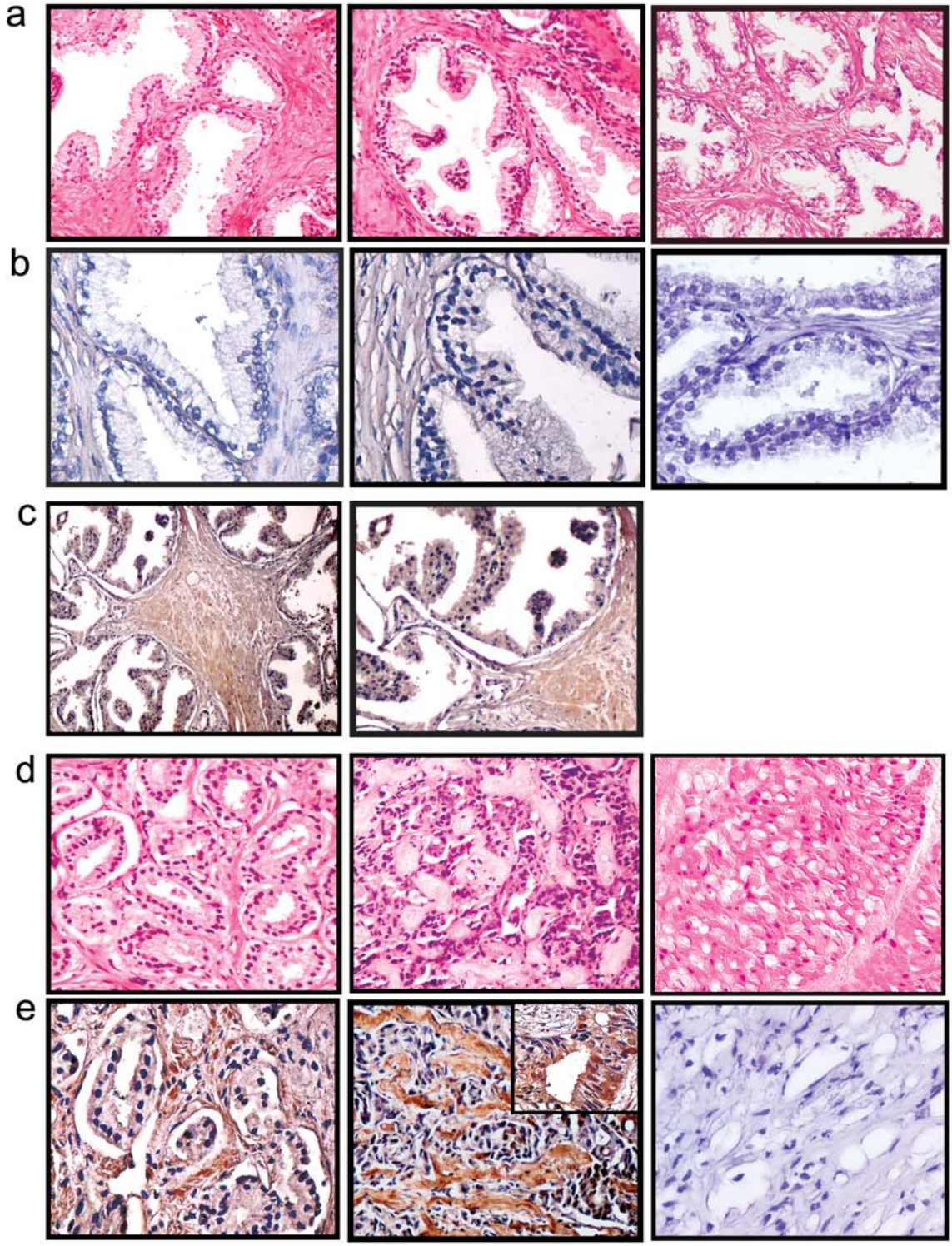

Figure 1. Expression of C17orf37 in human normal, benign prostatic hyperplasia (BPH) and prostate adenocarcinoma tissue specimens. Representative images of normal prostate gland (a, b -left), BPH (a, b -middle), prostate intraepithelial neoplasm (c), moderately differentiated (Gleason Score 6) (d, e - left) and poorly differentiated (Gleason Score 9) (d, e -middle) prostate carcinoma. Sections were stained with H & E (a, d) and ORF37 antibody (b, c, e). (b) Left, C17orf37 expression was found to be minimal in both normal prostate glands (*n=6*), (b) middle, in BPH prostate specimens (n=6), and (b) right, negative in IgG control. (c) C17orf37 staining in PIN glands show presence of protein in early stages of cancer progression. (e) Left, Moderately differentiated prostate adenocarcinoma tissue sections show increased expression of C17orf37 in both neoplastic glands and prostatic stroma (*n=15*), (e) middle panel, Poorly differentiated prostate adenocarcinoma tissue sections showed fusion of neoplastic glands with intense diffused C17orf37 immunostain *(n=12*), Inset shows C17orf37 expression in the prostatic glands in poorly differentiated carcinoma, and (e) right panel, shows negative staining in IgG control. All images are *100X* of original magnification except (c) left, which is *40X* of original magnification.

Figure 2

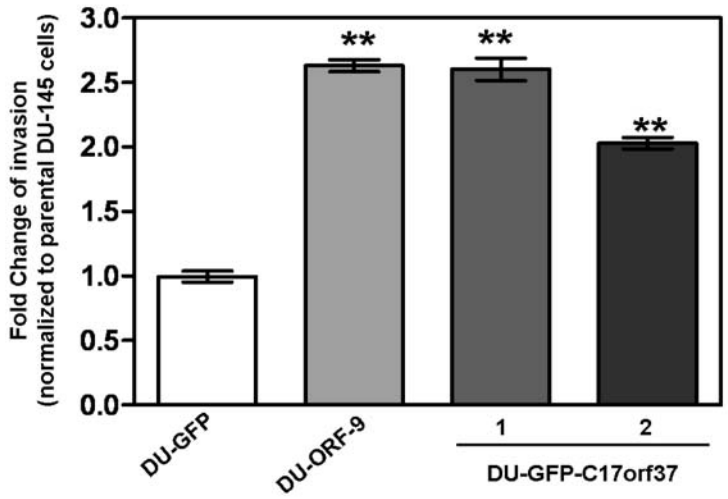
Fold Change of invasion
(normalized to parental DU-145 cells)
3.0
2.5
2.0
1.5
1.0
0.5
0.0
**
**
**
DU-GFP
DU-ORF-9
1
2
DU-GFP-C17orf37

Figure 2. Overexpression of C17orf37 increases invasive potential of DU-145 cells. Stable polyclonal population of DU-GFP (vector) and DU-GFP-C17orf37 (pool#1 and #2); stable randomly picked DU-ORF-9 (overexpressing GFP-C17orf37), and parental DU-145 cells were seeded onto matrigel coated tumor invasion chambers and allowed to migrate toward serum for 24 hours at 37°C. Fold change of invasion was calculated as described in supplementary materials and methods section. *Columns* are mean of three independent experiments; *bars*, SD. **, $P < 0.001$, relative to DU-GFP cells; statistical analysis included Student's *t* test for calculating significant differences within groups.

Figure 3

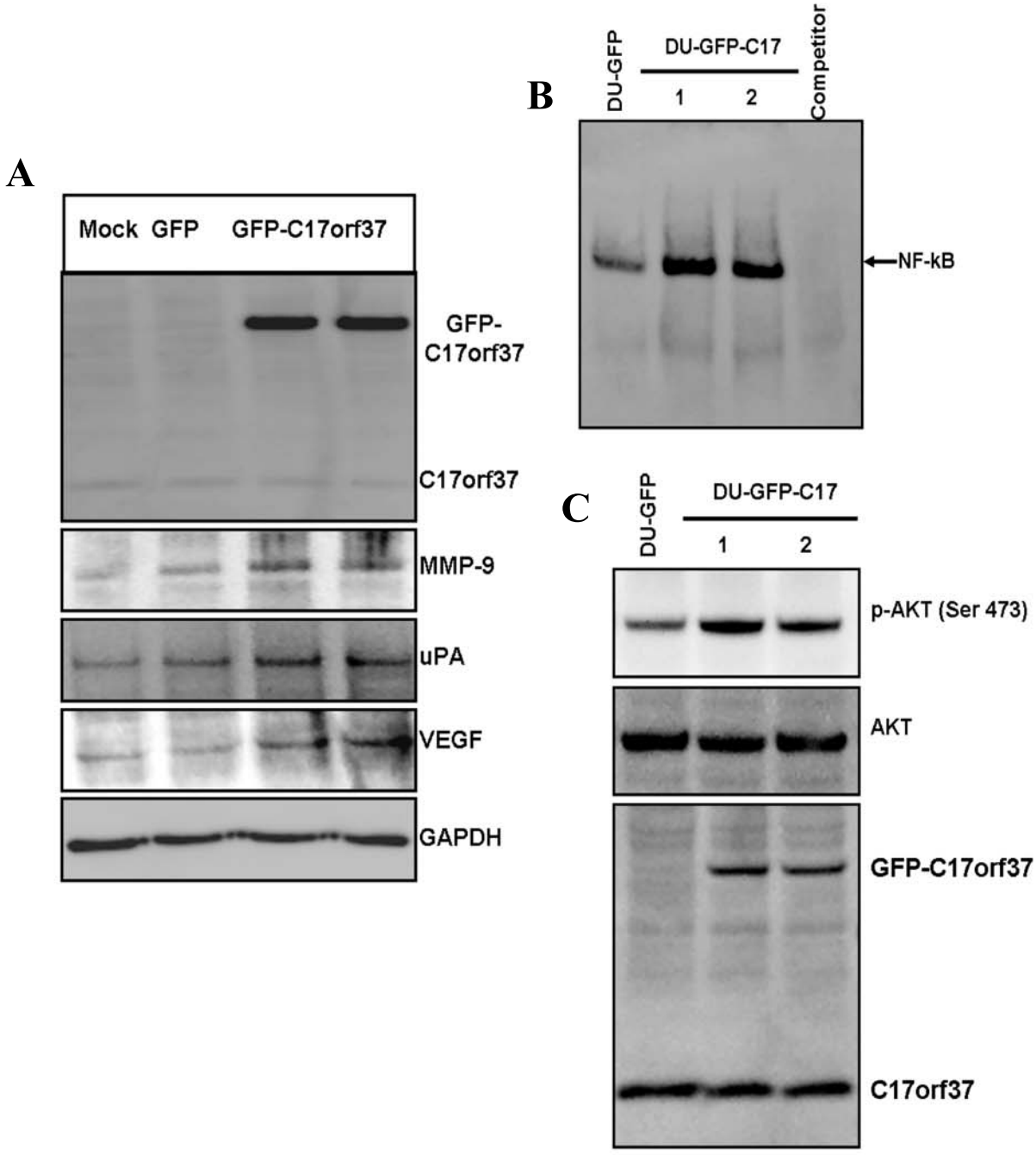
A
Mock
GFP
GFP-C17orf37
GFP-C17orf37
C17orf37
MMP-9
uPA
VEGF
GAPDH
B
DU-GFP
DU-GFP-C17
1
2
Competitor
NF-kB
C
DU-GFP
DU-GFP-C17
1
2
p-AKT (Ser 473)
AKT
GFP-C17orf37
C17orf37

Figure 3. (a) C17orf37 was over-expressed by transiently transfecting DU-145 cells with GFP-C17orf37 plasmid. Lipofectamine treated (mock) and GFP vector transfected were used as controls. Twnetyfour hours later total protein was isolated and 15 µg of protein was used to perform western immunoblot. Figures show expression of MMP-9, uPA and VEGF in mock-treated, GFP-vector only and GFP-C17orf37 treated DU-145 cells (in duplicate). All western blot images are representative of 4 independent experiments. (b) Western immunoblotting showing phospho-AKT and total AKT (top panel), and EMSA showing NF-κB DNA binding activity (bottom panel) in polyclonal populations overexpressing either DU-GFP (DU-145 stably expressing GFP vector) or DU-GFP-C17 (DU-145 stably expressing GFP-C17orf37) in two independent pools #1 and #2. Western blot and EMSA images are representative of three independent experiments.

Oncogene (2009) 28, 2860–2872

www.nature.com/onc

ORIGINAL ARTICLE

Novel gene *C17orf37* in 17q12 amplicon promotes migration and invasion of prostate cancer cells

S Dasgupta[1], LM Wasson[2], N Rauniyar[3], L Prokai[3], J Borejdo[3] and JK Vishwanatha[1,3]

[1]*Department of Biomedical Sciences and Institute for Cancer Research, University of North Texas Health Science Center, Fort Worth, TX, USA;* [2]*Department of Pathology, Harris Methodist Fort Worth Hospital, Fort Worth, TX, USA and* [3]*Department of Molecular Biology and Immunology, University of North Texas Health Science Center, Fort Worth, TX, USA*

***C17orf37/MGC14832*, a novel gene located on human chromosome 17q12 in the *ERBB2* amplicon, is abundantly expressed in breast cancer. C17orf37 expression has been reported to positively correlate with grade and stage of cancer progression; however the functional significance of C17orf37 overexpression in cancer biology is not known. Here, we show that C17orf37 is highly expressed in prostate cancer cell lines and tumors, compared to minimal expression in normal prostate cells and tissues. Cellular localization studies by confocal and total internal reflection fluorescence microscopy revealed predominant expression of C17orf37 in the cytosol with intense staining in the membrane of prostate cancer cells. RNA-interference-mediated downregulation of *C17orf37* resulted in decreased migration and invasion of DU-145 prostate cancer cells, and suppressed the DNA-binding activity of nuclear factor-κB (NF-κB) transcription factor resulting in reduced expression of downstream target genes matrix metalloproteinase 9, urokinase plasminogen activator and vascular endothelial growth factor. Phosphorylation of PKB/Akt was also reduced upon C17orf37 downregulation, suggesting C17orf37 acts as a signaling molecule that increases invasive potential of prostate cancer cells by NF-κB-mediated downstream target genes. Our data strongly suggest C17orf37 overexpression in prostate cancer functionally enhances migration and invasion of tumor cells, and is an important target for cancer therapy.**
Oncogene (2009) **28,** 2860–2872; doi:10.1038/onc.2009.145; published online 8 June 2009

Keywords: C17orf37; 17q12; prostate cancer; migration; invasion; NF-κB

Introduction

Prostate cancer is the most common type of cancer diagnosed in American men and is the second leading cause of cancer-related death in men (Pienta and Loberg, 2005). American Cancer Society estimates about 28 660 men will die of this disease in 2008. Most men diagnosed with prostate cancer can survive the primary localized tumor, but because of the metastasis-related disease, mortality rates remain extremely high. Metastasis of prostate cancer is facilitated by migration and invasion of malignant tumor cells from localized neoplastic tumors to distant organs like bone by cleavage of extracellular matrix (ECM) (Arya *et al*., 2006). Proteases that facilitate malignant cell migration and invasion by cleaving ECM proteins, such as matrix metalloproteinases (MMPs), cysteine proteases and serine proteases have been extensively studied (Sliva, 2004). Although the fundamental function of these proteases in prostate cancer cell migration, invasion and metastasis is clear, the underlying mechanism and regulation of these proteases to promote prostate cancer progression and invasion is vague.

Chromosome 17q12 contains multiple genes that are important in different forms of cancer. Recent genetic studies have projected 17q12 loci genes as an important risk factor in prostate cancer progression in selected individuals (Eeles *et al*., 2008; Sun *et al*., 2008). *ERBB2* located in the same amplicon is known to have significant function in prostate cancer progression and its expression correlates with poor hormone refractory prostate cancer in patients (Myers *et al*., 1994). *C17orf37* is a novel gene located in the same amplicon next to *ERBB2* in a tail-to-tail rearrangement, functional importance of which is presently unknown. *C17orf37* has been reported to be frequently amplified with *ERBB2* in breast tumor cells, however independent activation of *C17orf37* has been demonstrated in cell lines expressing low levels of *ERBB2* (Evans *et al*., 2006). C17orf37 protein is abundantly expressed in breast tumor cells and clinical tissues, with reduced or limited expression in 38 different normal tissues (Evans *et al*., 2006). C17orf37 expression positively correlates with grade and stage of breast cancer, and increased expression has been shown in patients with breast to liver and lungs metastasis (Evans *et al*., 2006). This suggests C17orf37 protein may be an important mediator of cancer cell metastasis. However, to establish C17orf37 as a biomarker and therapeutic target for cancer treatment, it is utmost important to explore the functional importance of this novel protein.

Correspondence: Dr JK Vishwanatha, Department of Molecular Biology and Immunology, Graduate School of Biomedical Sciences, University of North Texas Health Science Center, 3500 Camp Bowie Boulevard, Fort Worth, TX 76107, USA.
E-mail: jvishwan@hsc.unt.edu
Received 24 September 2008; revised 17 April 2009; accepted 6 May 2009; published online 8 June 2009

We demonstrate C17orf37 expression is enhanced in prostate cancer cells and tissues specimens. We also observed the cellular localization of C17orf37 in prostate cells by confocal microscopy and finally by knockdown and overexpression studies, we demonstrate C17orf37 significantly contributes to the migration and invasion of prostate cancer cells. Our results clearly indicate C17orf37 as a critical cancer-specific protein promoting tumor cell invasion by enhancing secretion of urokinase plasminogen activator (uPA), MMP-9 and vascular endothelial growth factor (VEGF) through nuclear factor-κB (NF-κB) pathway.

Results

Increased expression of C17orf37 in prostate cancer cells
To investigate C17orf37 expression in prostate cancer, we analysed mRNA expression of *C17orf37* in a panel of prostate cancer cell lines including androgen-independent DU-145 and PC-3, and in an LNCaP cell line prostate cancer progression model consisting of androgen-dependent LNCaP-R and androgen-independent LNCaP-UR (Rothermund *et al*., 2002) by q-RT–PCR (Figure 1a) and reverse transcription (RT)–PCR (Supplementary Figure 1). We found high levels of *C17orf37* mRNA expression in all the prostate cancer cell lines investigated, whereas expression in both the normal prostate epithelial cell lines HPV18 C-1 and PWR-1E was relatively low (Figure 1a). To analyse the protein expression of C17orf37 in prostate carcinoma cells, we first determined the specificity of the anti-C17orf37 antibody (ORF37) using recombinant GST-C17orf37 protein. ORF37 antibody immunoreacts with both GST-C17orf37 (39 kDa) and GST-tag cleaved purified recombinant C17orf37 protein of 12 kDa size (Figure 1b). To verify the 12 kDa band is indeed C17orf37 protein, we analysed the protein sequence by tandem mass spectrometry. As shown by high-resolution ESI-FTICR analysis (Supplementary Figure 2), the molecular weight of the intact recombinant protein was 11 918 Da and matched 54% amino-acid sequence coverage of C17orf37 (Figure 1c).

To find any possible change in C17orf37 protein expression from androgen dependency to independency, we examined two additional prostate cancer cell lines LNCaP-RF, a fast growing androgen-responsive LNCaP cell line (Rothermund *et al*., 2002) and LNCaP/C4-2 (LNC4-2), a subline derived from parental LNCaP cells that acquired phenotypes of androgen independence (Thalmann *et al*., 1994; Wu *et al*., 1994). Among metastatic prostate cancer cell lines, DU-145 showed higher C17orf37 expression compared to PC-3 (Figure 1d), whereas *in vitro* LNCaP prostate cancer progression models—UR, RF and R along with LNCaP C4-2—showed similar level of protein expression (Figure 1d), suggesting C17orf37 expression persists both in androgen-dependent and -independent states of prostate cancer. As with our observations made at the mRNA level, normal prostate epithelial cell lines HPV18 C-1 and PWR-1E showed undetectable expression of C17orf37 protein (Figure 1d). These data indicated that expression of C17orf37 persists throughout prostate cancer disease progression, both in early stages of androgen dependency to late stages of androgen independency, with minimal expression in normal prostate cell lines.

C17orf37 is overexpressed in high-grade neoplastic glands and stroma of prostate adenocarcinoma
To determine the expression of C17orf37 in normal and cancerous prostate tissues, we examined C17orf37 expression in archival formalin-fixed paraffin-embedded prostate specimens by immunohistochemistry. The hematoxylin and eosin (H&E)-stained specimens were classified into normal, benign prostatic hyperplasia (BPH), moderately differentiated prostate adenocarcinoma and poorly differentiated prostate adenocarcinoma (Banerjee *et al*., 2003; Figures 2a and d) by anatomic pathologists. Gleason scores of the prostate carcinoma tissues ranged from 6 to 10, thus no well-differentiated prostate adenocarcinoma specimens (Gleason score 2–4) were available for our study. In both normal prostate glands (Figure 2b, left) and transurethral resection of the prostate BPH specimens (Figure 2b, middle), C17orf37 staining was minimal in prostatic glands and stroma. Prostate intraepithelial neoplasm (PIN) showed moderately increased staining of C17orf37 (Figure 2c) compared to normal or BPH glands in the same section. However, in moderately differentiated specimens C17orf37 expression was found to be intense in the neoplastic glands and stromal cells surrounding the glands (Figure 2e, left). Strong C17orf37 expression was found throughout the poorly differentiated prostate cancer sections with intense diffused stain in the stroma around the malignant cell mass and invasive edges (Figure 2e, middle). C17orf37 expression was intense in the fused prostatic glands of poorly differentiated prostatic cancer (Figure 2e, 'inset' middle). The isotype controls (IgG) for each specimen did not show immunoreactivity (Figures 2b and e, right). Taken together, immunohistochemical detection of C17orf37 protein showed prevalent expression in the higher grades of prostate adenocarcinoma with densely stained malignant cells compared to either low or null expression in both normal and BPH specimens.

Subcellular localization of C17orf37 in prostate cancer cells
We investigated the intracellular localization of C17orf37 protein in prostate cells. In DU-145 and LNCaP cells, western immunoblot of cellular fractions (Figure 3a) and immunocytochemical detection by confocal microscopy (Figure 3b, left, DU-145; right, LNCaP) showed endogenous expression of C17orf37 predominantly in the cytosol. Transient transfection of GFP-C17orf37 in DU-145 (Figure 3c, left), LNCaP (Figure 3c, middle) and HPV18 C-1 (Figure 3c, right) prostate cells also showed similar pattern of C17orf37 expression. Endogenous C17orf37 and GFP-C17orf37

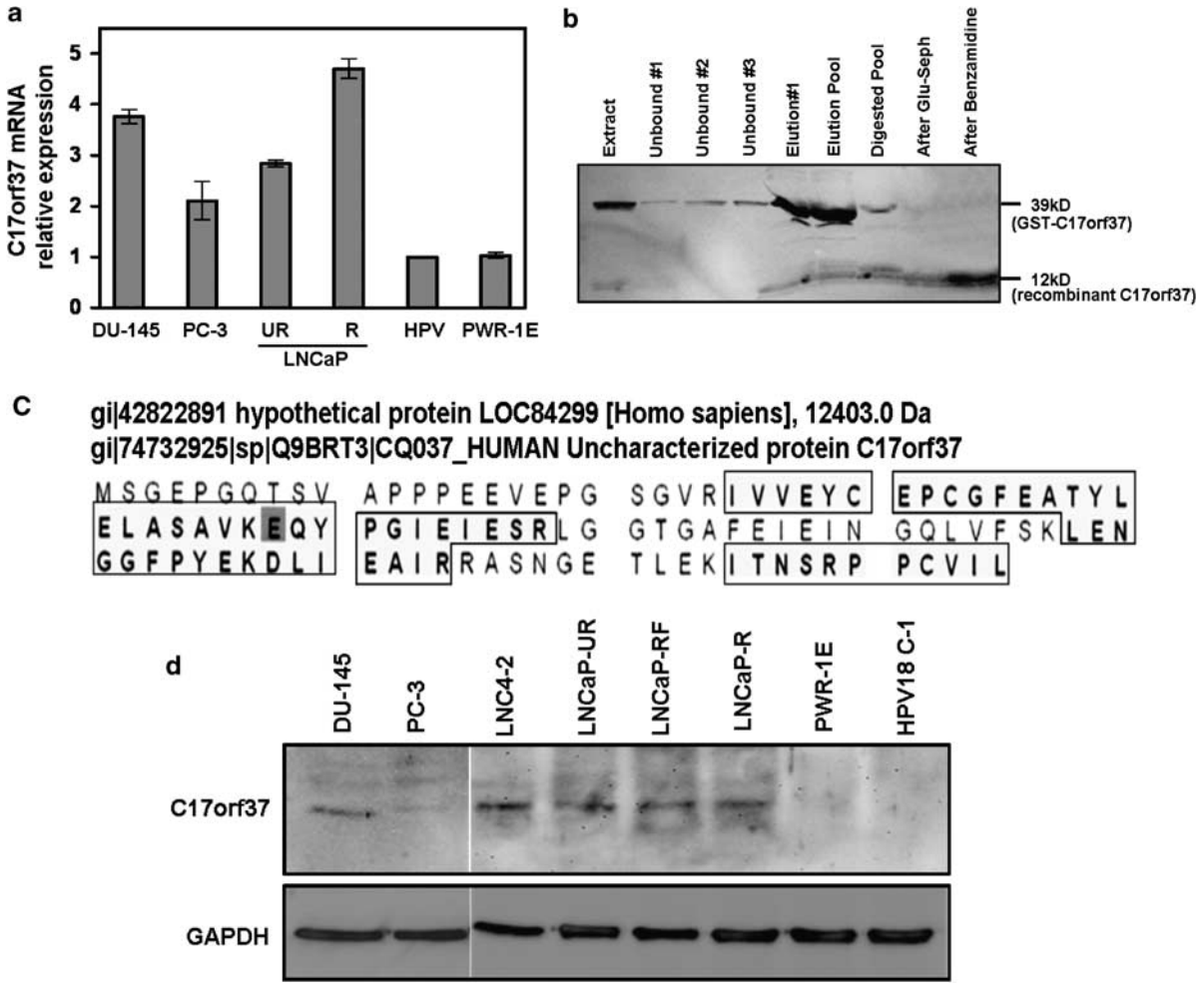

Figure 1 *C17orf37* mRNA and protein expression in human prostate cancer cells. (**a**) *C17orf37* mRNA expression was analysed by real-time PCR in prostate cancer cell lines DU-145, PC-3, LNCaP-UR and LNCaP-R, and normal prostate epithelial cell line HPV18 C-1 and prostate-derived cell line PWR-1E. Housekeeping gene *β-actin* was used as an internal control. (**b**) Western immunoblot showing the expression of GST-C17orf37 protein that was purified and thrombin cleaved to generate recombinant C17orf37 protein. (**c**) Summary of LC/ESI-MS/MS analysis for the predicted C17orf37 after tryptic digestion (4 unique peptides and 54% sequence coverage, 62 out of 115 amino-acid residues shown; the box indicates the amino-acid residues covered and gray highlight denotes conversion of E to <E upon proteolytic digestion). (**d**) C17orf37 protein was analysed by western immunoblot in a panel of prostate cancer cell lines including DU-145, PC-3 and LNC4-2 (androgen independent); LNCaP progression model LNCaP-UR, LNCaP-RF and LNCaP-R (from androgen independent to dependent); and, normal prostate epithelial cell line HPV18 C-1 and PWR-1E. Housekeeping gene glyceraldehyde-3-phosphate dehydrogenase (*GAPDH*) served as loading control. Expression of C17orf37 protein was higher in prostate cancer cells compared to normal prostate cells.

localized primarily in the cytoplasm of the transfected cells, densely in the perinuclear area around the membrane (white arrows) and less in the nucleus (Figures 3b and c). Localization was similar in both C17orf37-positive prostate cancer cells DU-145 and LNCaP, and a null C17orf37 HPV18 C-1 (Figure 3c). To determine whether C17orf37 is a membrane-bound protein, we performed total internal reflection fluores-

Figure 2 Expression of C17orf37 in human normal, benign prostatic hyperplasia (BPH) and prostate adenocarcinoma tissue specimens. Representative images of normal prostate gland (**a**, **b**, left), BPH (**a**, **b**, middle), prostate intraepithelial neoplasm (**c**), moderately differentiated (Gleason score 6) (**d**, **e**, left) and poorly differentiated (Gleason score 9) (**d**, **e**, middle) prostate carcinoma. Sections were stained with hematoxylin and eosin (H&E) (**a**, **d**) and ORF37 antibody (**b**, **c** and **e**). (**b**) Left, C17orf37 expression was found to be minimal in both normal prostate glands ($n=6$); (**b**) middle, in BPH prostate specimens ($n=6$) and (**b**) right, negative in IgG control. (**c**) C17orf37 staining in PIN glands shows presence of protein in early stages of cancer progression. (**e**) Left, moderately differentiated prostate adenocarcinoma tissue sections show increased expression of C17orf37 in both neoplastic glands and prostatic stroma ($n=15$); (**e**) middle panel, poorly differentiated prostate adenocarcinoma tissue sections showed fusion of neoplastic glands with intense diffused C17orf37 immunostain ($n=12$), inset, C17orf37 expression in the prostatic glands in poorly differentiated carcinoma and (**e**) right panel, negative staining in IgG control. All images are $\times 100$ of original magnification except (**c**) left, which is $\times 40$ of original magnification.

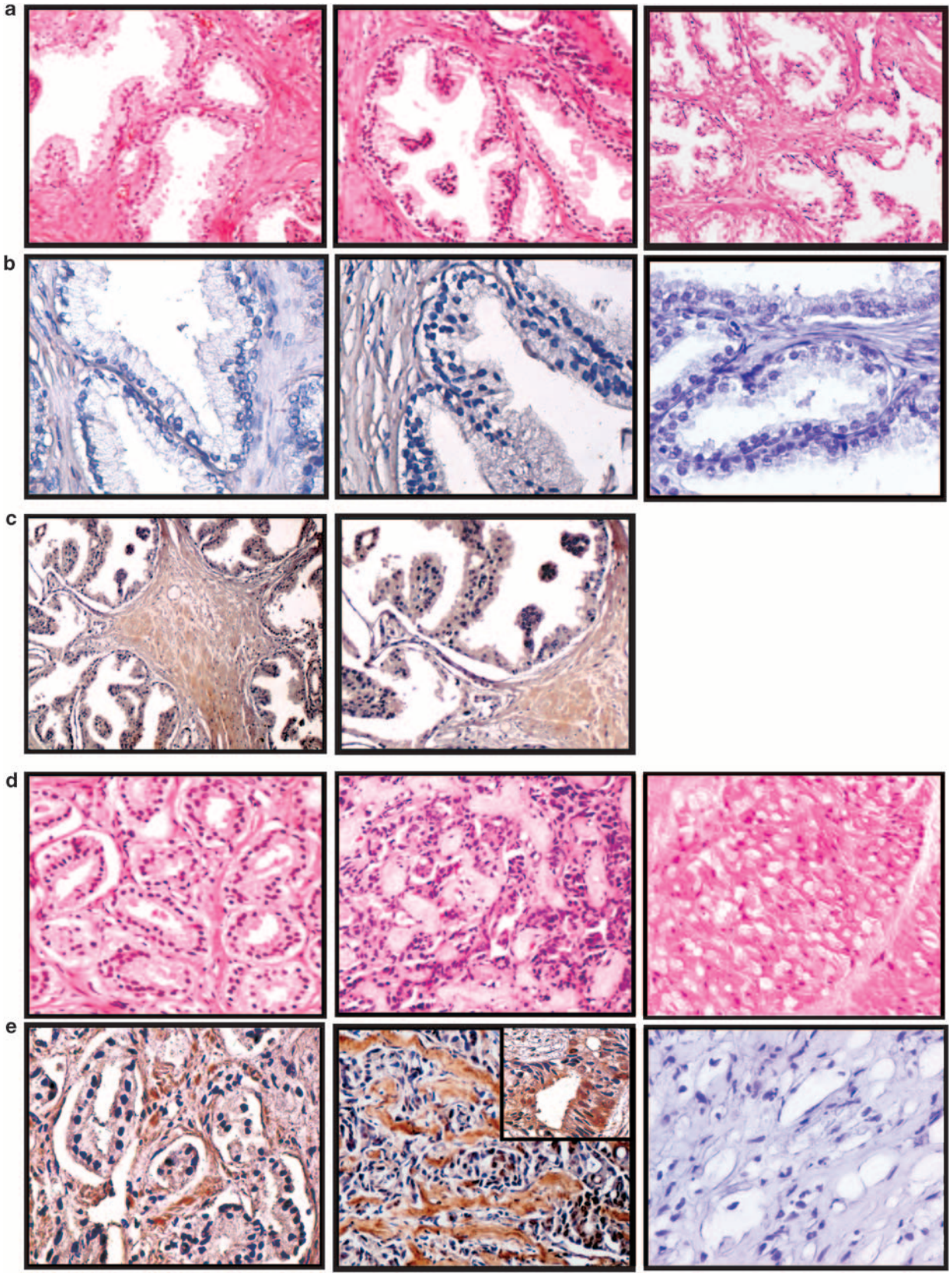
a
b
c
d
e

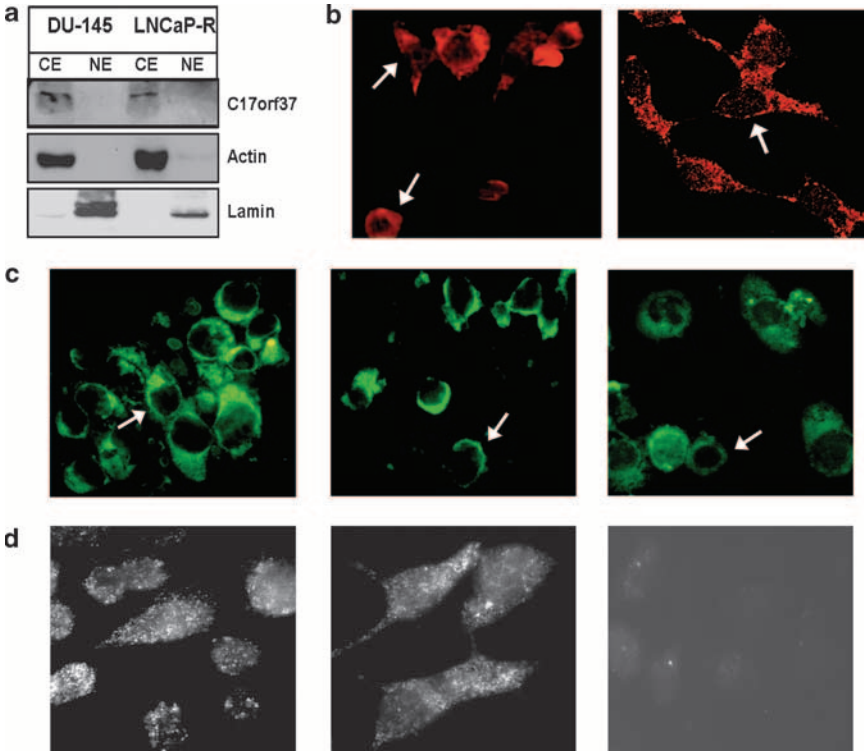

Figure 3 Subcellular localization of C17orf37 in human prostate cancer cell lines. (**a**) Subcellular fractionation followed by western immunoblot showing endogenous expression of C17orf37 in the cytosolic fractions of DU-145 and LNCaP-R prostate cancer cells. The purity of the cytosolic (CE) and nuclear extracts (NE) was determined using cytosolic marker protein actin and nuclear protein lamin. (**b**) Immunofluorescent staining of endogenous C17orf37 expression in DU-145 (middle) and LNCaP-R (right) prostate cancer cells. Confocal images show intense C17orf37 staining in the cytosolic compartment with dense spots in the membrane. Original magnification, $\times 40$. (**c**) GFP-C17orf37 construct was transiently transfected in DU-145 (left), LNCaP (middle) and HPV18 C-1 cells (right). The cells were then fixed and imaged by confocal microscopy. GFP-C17orf37 was visualized as green fluorescent signals mostly in the cytosolic area predominantly in the membrane. Original magnification, $\times 40$. (**d**) DU-145 (left and right) and LNCaP-R cells (middle panel) were grown in coverslips, fixed, unpermeabilized and treated with anti-C17orf37 (left and middle) or anti-tubulin (right) antibody. Coverslips were mounted on special total internal reflection fluorescence (TIRF) coverslips as mentioned in the Materials and methods section. Slides were visualized by TIRFM. Spots as seen in the images depict the membrane localization of C17orf37 in prostate cancer cells. Original magnification, $\times 60$ oil immersion. White arrows indicate membrane localization of C17orf37 in prostate cancer and noncancerous cells.

cence microcopy (TIRFM) to monitor membrane localization of C17orf37. In the TIRFM, the evanescent wave produced by the visible light at the cell/substratum interface penetrates only 100–200 nm with decaying intensity with the distance, allowing detection of protein molecules associated with the plasma membrane (Axelrod, 2001). DU-145 and LNCaP (Figure 3d, left and middle, respectively) cells labeled with ORF37 antibody tagged to Alexa fluorophore-568 showed numerous dense spots of C17orf37 protein in the membrane region (Figure 3d). We used intracellular cytoskeletal protein tubulin as a control for our experiments, but TIRFM failed to image tubulin protein molecules on the membrane (Figure 3d, right). These results indicated that C17orf37 is a cytosolic protein with predominant membrane localization in prostate cancer cells.

Expression of C17orf37 enhances the in vitro *invasive and migratory potential of prostate cancer cells*

Our results show expression of C17orf37 is higher in advanced prostate adenocarcinomas (Gleason grades: 6 and 9) compared to normal prostate tissues (Figures 2b and e). Metastases of malignant cells to distant tissues or organs are mediated by cellular migration, invasion and proteolytic activity that degrade tissue barrier (Sliva, 2004). To investigate the function of C17orf37 in prostate cancer cell migration, we studied the effect of C17orf37 downregulation on the migratory potential of DU-145 cells. Using gene-specific siRNA at varying concentrations, we blocked the endogenous expression of C17orf37 in DU-145 cells (Figure 4a). An *in vitro* agarose gel bead assay was performed with C17orf37 knocked-down DU-145 cells, to determine the dose-dependent effect of siRNA-C17orf37 on DU-145 cell migration. As shown in Figure 4b, siRNA-C17orf37 treatment (Figure 4b, III–V) reduced the number of DU-145 cells that could migrate out of the agarose gel bead into the medium compared to wild-type or control-siRNA-treated (Figure 4b, I–II) cells. siRNA–C17orf37 treatment at 100 nM resulted in $\sim$10-fold decrease in migration of DU-145 cells ($P<0.0001$) compared to control wild-type cells (Figure 4c). *In vitro* tumor invasion assay also showed reduced invasive ability of

DU-145 cells treated with siRNA-C17orf37 (Figure 4d). To verify expression of C17orf37 has a dominant effect on tumor cells invasion, we assessed invasiveness of DU-145 and PC-3 cells overexpressed with GFP-C17orf37. C17orf37-positive DU-145 prostate cancer cells showed ~1.8-fold increase, whereas PC-3, with low endogenous C17orf37 expression, showed ~1.75-fold increase in invasion compared to respective controls (Figure 4e). Stable overexpression of GFP-C17orf37 construct in DU-145 cells (DU-GFP-C17orf37) dramatically increased the invasiveness ~2.6- and ~1.95-fold compared to parental DU-145 cells (Supplementary

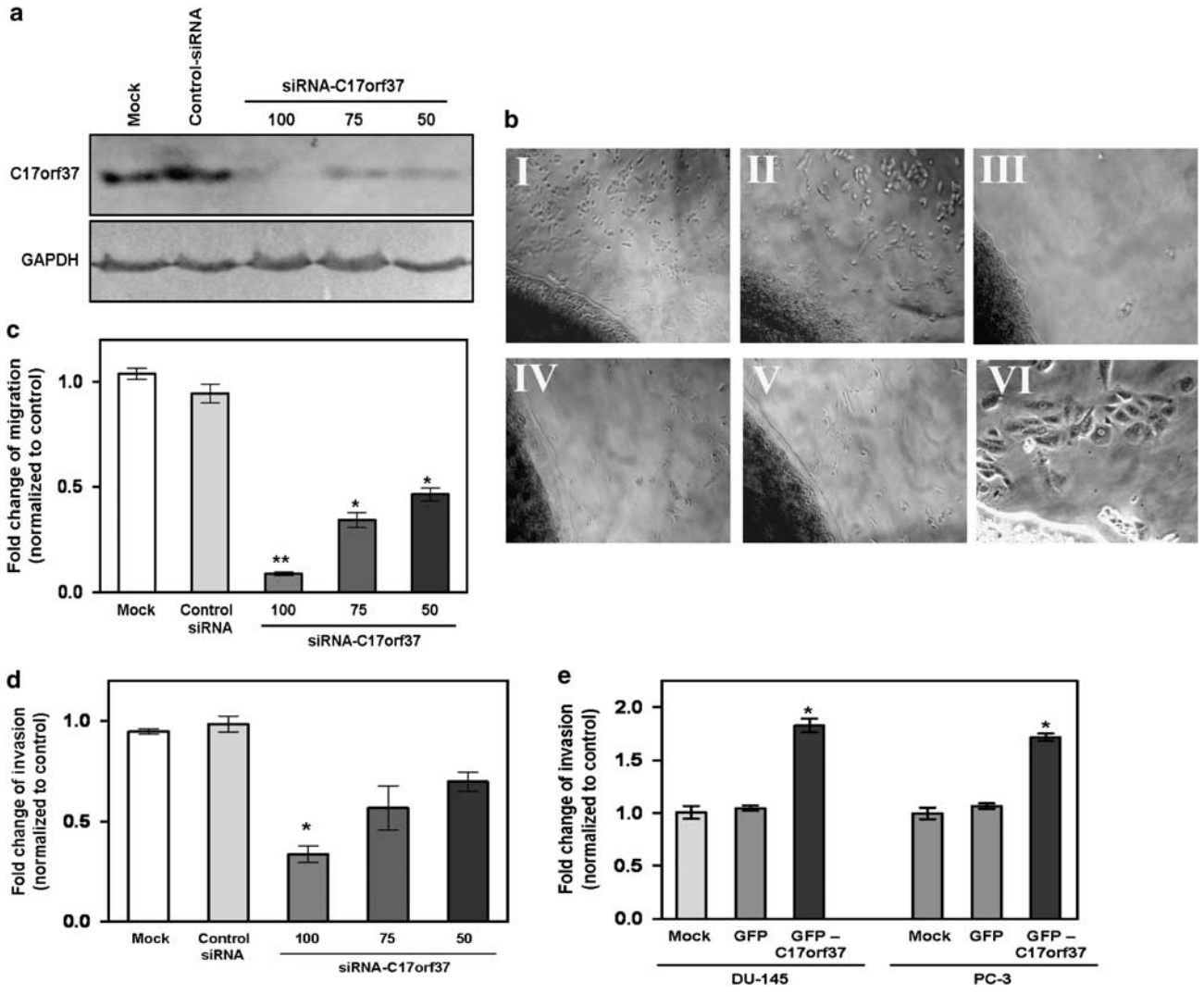

Figure 4 C17orf37 expression regulates migration and invasion of prostate cancer cells. (**a**) DU-145 cells were transfected with transfection media alone (mock); non-targeting scrambled siRNA (control siRNA); and 100, 75 and 50 nM doses of C17orf37-specific siRNA. Following 48 h of transfection, C17orf37 protein knockdown was confirmed by western immunoblot using ORF37 antibody and compared to glyceraldehyde-3-phosphate dehydrogenase (GAPDH). Blot is representative image of four independent experiments. (**b**) At 48 h of post-transfection DU-145 cells were mixed in low melting agarose and growth medium, and plated on fibronectin-coated plates to form a semisolid gel bead. Representative pictures taken after 36 h show the number of DU-145 cells that migrate out of the gel beads treated with—I, transfection medium only (mock); II, nontargeting siRNA (control siRNA); III, 100 nM of C17orf37-specific siRNA; IV, 75 nM of C17orf37 siRNA; V, 50 nM of C17orf37-specific siRNA and VI, VI shows the normal morphology of the DU-145 cells that migrate out of the agarose gel beads. (**c**) Graphical representation of fold change in DU-145 prostate cancer cell migration compared to control (untreated) wild-type cells. (**d**) DU-145 cells transfected with mock, nontargeting control siRNA, and 100, 75 and 50 nM siRNA-C17orf37 were incubated for 48 h. After the transfection phase, DU-145 cells were seeded onto Matrigel-coated BD BioCoat Tumor Invasion system and allowed to migrate toward 10% serum for 24 h. Fold change of invasion was calculated as described in Materials and methods section. (**e**) DU-145 and PC-3 cells were transiently transfected with transfection media alone (mock), EGFP-C1 vector only (GFP) and EGFP-C17orf37 plasmid (GFP-C17orf37). After 24 h, cells were seeded onto Matrigel-coated tumor invasion chambers and allowed to migrate toward serum for 24 h at 37 °C. Fold change of invasion and migration was calculated as described in Materials and methods section. Columns (**c**–**e**) are mean of three independent experiments; bars, s.d. $^{**}P<0.0001$ and $^{*}P<0.05$, relative to mock treatment of cells; statistical analysis included Student's *t*-test for calculating significant differences within groups.

Figure 3), indicating overexpression of C17orf37 protein leads to increased invasive behavior in prostate cancer cells.

Downregulation of C17orf37 results in reduced expression of MMP-9, uPA and VEGF by lowering NF-κB DNA-binding activity in DU-145 prostate cancer cells

Migration and invasion of malignant cells is facilitated by specific proteases like MMPs (such as MMP-9) and serine proteases (such as uPA) that degrade the ECM (Sliva, 2004). During prostate cancer progression these molecules are found to be predominantly upregulated to facilitate migration and invasion (Wilson and Sinha, 1993; Lokeshwar, 1999; Wilson *et al*., 2004; Helenius *et al*., 2006; Li and Cozzi, 2007). Prostate cancer cells also secrete high levels of growth factors like VEGF, which is an important mediator of angiogenesis, proliferation and migration (Hicklin and Ellis, 2005). To investigate whether C17orf37 protein has any effect on the metastasis-related genes, we knocked down endogenous C17orf37 in DU-145 cells and analysed expression of several genes that facilitate prostate cancer metastasis and promote ECM cleavage. We observed suppression of endogenous C17orf37, simultaneously reduced MMP-9, uPA and VEGF expression as measured by RT–PCR (Figure 5a) and western immunoblot (Figure 5b) compared to nontargeting siRNA (control siRNA). To determine if C17orf37 expression increases MMP-9, uPA and VEGF protein in prostate cancer cells, we overexpressed C17orf37 in DU-145 cells by transient transfection of GFP-C17orf37 plasmid. As shown in Figure 5c, western immunoblot confirmed overexpression of C17orf37 increases endogenous MMP-9, uPA and VEGF protein compared to vector-treated cells. Interestingly, silencing of C17orf37 in DU-145 prostate cancer cells resulted in reduced mRNA expression of both the isoforms of VEGF ($VEGF_{165}$ and $VEGF_{121}$; Figure 5a). $VEGF_{121}$ isoform is rapidly secreted and freely diffuses into the tissues, whereas $VEGF_{165}$ the potent isoform functionally active in most angiogenic states (Connolly and Rose, 1998; Woolard *et al*., 2004) was found to be regulated by C17orf37 (Figures 5b and c). To quantitate the relative amount of secreted VEGF (both the isoforms) and MMP-9 we performed enzyme-linked immunosorbent assay (ELISA) of conditioned media from DU-145 cells overexpressed or depleted C17orf37 protein. Our results show that secreted MMP-9 and VEGF protein are significantly altered due to C17orf37 expression compared to respective controls (Figure 5d).

MMP-9, *uPA* and *VEGF* genes are transcriptionally upregulated by NF-κB, which is constitutively active in prostate cancer cells (Suh and Rabson, 2004). We performed electrophoretic mobility shift assay (EMSA) to evaluate the DNA-binding activity of NF-κB in C17orf37-silenced DU-145 cells. Our results indicate increasing concentration of C17orf37-specific siRNA effectively inhibited NF-κB DNA-binding activity in a dose-dependent manner (Figure 6a). These results show that C17orf37 increases migration and invasion in prostate cancer by NF-κB-mediated genes *MMP-9*, *uPA* and *VEGF*. In prostate cancer cells, constitutive activation of NF-κB is mediated by upstream protein kinase B (PKB/Akt) (Fresno Vara *et al*., 2004), so we performed western immunoblot to detect the levels of phosphorylated Akt (p-Akt) and total Akt. p-Akt is the active form of the protein that cascades the intracellular signaling and our results show blocking of C17orf37 by siRNA dramatically reduced p-Akt level in DU-145 cells (Figure 6b). C17orf37-specific siRNA (100 nM) treatment abolished 80% phosphorylation of Akt in DU-145 cells (Supplementary Figure 4) whereas the total Akt expression was constant when normalized to loading control glyceraldehyde-3-phosphate dehydrogenase (GAPDH). We also observed reduction in the phosphorylated form of ERK1/2 compared to total ERK1/2 (Figure 6b), however the extent of reduction was not significant when compared to Akt activation (Supplementary Figure 4). To validate our observation, we measured p-Akt/Akt level and NF-κB DNA-binding activity in DU-145 cells stably overexpressing GFP-C17orf37 (DU-GFP-C17), and as expected phosphorylation of Akt and NF-κB activity was significantly higher in C17orf37-overexpressed cells compared to vector control cells (DU-GFP) (Figure 6c). These results demonstrate that C17orf37 mediates prostate cancer cell migration and invasion through NF-κB downstream target genes *MMP-9*, *uPA* and *VEGF*.

Discussion

C17orf37 is a novel gene located on human chromosome 17q12, in the 'hot spot locus of cancer' that contains multiple genes that have been shown to be involved in the progression of cancer. *C17orf37* gene is 505 nucleotides from *ERBB2* oncogene, which has been demonstrated as an important factor for development of hormone refractory prostate cancer (Berger *et al*., 2006). Although *C17orf37* overexpression in breast cancer has been linked with genomic amplification of Her-2/*neu* locus, recent report has confirmed overexpression of *C17orf37* in Her-2/*neu*-negative breast cancer patients and breast tumor cell lines, suggesting independent transcriptional control mechanisms for *C17orf37* (Evans *et al*., 2006). In the present study, we show that C17orf37 expression is consistently higher in both androgen-dependent and -independent prostate cancer cell lines and clinical prostate cancer tissues examined, compared to either low or null expression in normal and BPH prostate cells and tissues (Figures 1 and 2). In clinical prostate cancer specimens, higher Gleason-scored tumors showed increased C17orf37 expression compared to lower scores, suggesting C17orf37 expression may increase with grade and stage of cancer. However, the small number of established prostate cancer cell lines does not show significant changes in C17orf37. A larger study with more patient population will be necessary to establish C17orf37 as a biomarker for prostate cancer progression. Our data provide the

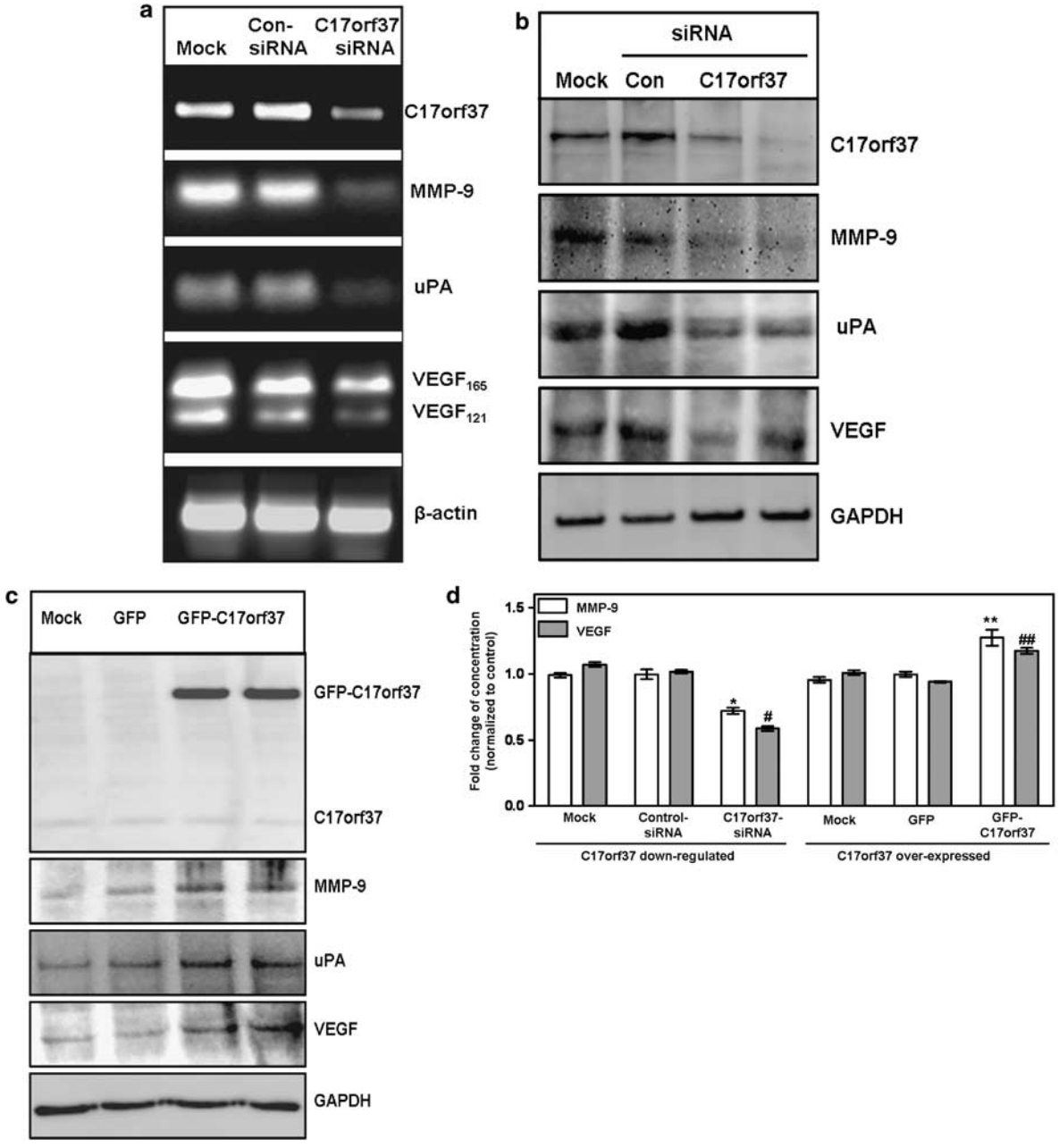

Figure 5 siRNA-mediated silencing of *C17orf37* results in the downregulation of matrix metalloproteinase 9 (*MMP-9*), urokinase plasminogen activator (*uPA*) and vascular endothelial growth factor (*VEGF*) expression. DU-145 cells were transiently transfected with transfection media (DharmaFECT) alone (mock), nontargeting siRNA (control siRNA) and SMART pool siRNA specific to C17orf37 (100 nM). (**a**) After 70 h total RNA was isolated and the mRNA expression of MMP-9, uPA and VEGF was analysed by reverse transcription (RT)–PCR. Housekeeping gene *β-actin* served as internal control. (**b**) At 96 h after transfection total protein was isolated and 30 μg of protein was used to perform western immunoblot. Expression of MMP-9, uPA and VEGF protein was analysed in mock, control siRNA and C17orf37-specific siRNA (100 nM; in duplicate)-treated DU-145 prostate cancer cells. (**c**) C17orf37 was overexpressed by transiently transfecting DU-145 cells with GFP-C17orf37 plasmid. Lipofectamine-treated (mock) and green fluorescent protein (GFP) vector transfected cells were used as controls. After 24 h total protein was isolated and 15 μg of protein was used to perform western immunoblot. Figures show expression of MMP-9, uPA and VEGF in mock-treated, GFP vector only and GFP-C17orf37-treated DU-145 cells (in duplicate). All western blot images are representative of four independent experiments. (**d**) Enzyme-linked immunosorbent assays (ELISA) of conditioned media from DU-145 cells treated as in (**b**) and (**c**) were used to estimate MMP-9 and VEGF. Fold change of concentration was determined by a ratio of quantitative values of MMP-9 (ng/ml per 10^5 cells) and VEGF (pg/ml per 10^5 cells) in experimental group to the control group. Columns, mean of four independent experiments; bars, s.d. $^*P<0.005$ relative to mock (DharmaFECT) treated (MMP-9); $^{\#}P<0.005$ relative to mock treated (VEGF); $^{**}P<0.05$ relative to mock (Lipofectamine) treated (MMP-9) and $^{\#\#}P<0.05$ relative to mock treated (VEGF); statistical analysis included Student's *t*-test for calculating significant differences within groups.

first evidence that C17orf37 expression positively correlates with the migratory and invasive potential of metastatic prostate cancer cells and thereby can be regarded as a potential biomarker for the disease progression. This is the first report delineating the role, functional significance and a proposed mechanism through which this novel gene *C17orf37* governs prostate cancer progression.

C17orf37 gene encodes a protein (accession no. NP_115715) of 115 amino acids with a molecular weight of ~12 kDa (Figure 1c; Supplementary Figure S2) that has no sequence similarity with any known genes or proteins (Evans *et al*., 2006; Kauraniemi and Kallioniemi, 2006). By immunoconfocal microscopy, TIRFM and cellular fractionation studies we show that C17orf37 is predominantly a cytosolic protein, densely located in the cell membrane (Figure 3). In migrating prostate cancer cell, C17orf37 protein primarily localizes to the leading edge of cell (Supplementary Figure 5). Careful analysis of the C17orf37 protein sequence (Figure 1c) revealed a 'CaaX' prenylation motif comprising of last four amino acids 'CVIL' at the C-terminal end. 'CaaX' group of proteins are either farnesylated or geranylgeranylated by enzymes farnesyltransferase and geranylgeranyl transferase type I (GGTase-I), respectively. If 'X' is leucine, protein is preferentially modified by GGTase-I enzyme (Fu and Casey, 1999), suggesting C17orf37 translocation to the membrane may be mediated by GGTase-I. Pre-PS (prenylation prediction suite) predicted C17orf37 to be prenylated preferentially by the enzyme GGTase-I with a P-value = 0.00049 (Maurer-Stroh and Eisenhaber, 2005) and this idea was also supported by a recent report (Evans *et al*., 2006).

'CaaX'-type prenylated proteins are primarily located at the cytoplasmic face of cellular membranes and in cancer cells these proteins are found to have significant function in oncogenic transformation, cytoskeletal organization, cellular proliferation, migration, invasion and metastasis (Virtanen *et al*., 2002; Winter-Vann and Casey, 2005; Kelly *et al*., 2006). By RNAi-mediated *C17orf37* gene silencing and also by overexpressing C17orf37 in prostate cancer cells, we successfully established that C17orf37 regulates migration and invasion (Figure 4). Even in patients with metastasis of breast cancer to liver and lungs, abundant expression of C17orf37 protein has been reported (Evans *et al*., 2006). Migration and invasion of cancer cells are the hallmark of malignant neoplastic proliferation beyond the vascular boundaries facilitated by ECM cleavage by proteolytic enzymes. SiRNA mediated knockdown of C17orf37 in DU-145 cells, reduced mRNA and protein expression of important proteolytic enzymes MMP-9 and uPA, and potent angiogenic molecule VEGF (Figure 5), suggesting C17orf37 may act as an important upstream signaling molecule enhancing the transcription of these genes. uPA binding to its receptor uPA-R at the cell surface converts inactive plasminogen to active plasmin, and thereby cleaves ECM proteins inducing migration and invasion of malignant cells (Li and Cozzi, 2007). MMP-9 specifically cleaves ECM proteins like gelatin, collagen I and IV, vitronectin and fibronectin resulting in metastatic dissemination of malignant cells (Price *et al*., 1997). In prostate cancer development, angiogenic growth factor VEGF has key function in promoting tumor growth and metastatic progression of the disease. MMP-9, uPA and VEGF have been reported to be overexpressed in invasive prostate cancer (Wilson and Sinha, 1993) and are positively correlated with poor prognosis (Sheng, 2001). We show here that by modulating C17orf37 expression in DU-145 metastatic prostate cancer cells, expression of these key molecules is significantly reduced, thereby inhibiting prostate cancer cell migration and invasion.

In invasive prostate cancer cells, increased expression of *MMP-9*, *uPA* and *VEGF* genes is regulated by transcriptional activation of NF-κB (Huang *et al*., 2001). Activation of NF-κB is due to increased activity of upstream kinase IKK complex that greatly reduces the half-life of the inhibitory IκBα, thereby inducing nuclear localization of NF-κB (Suh and Rabson, 2004). Knockdown of C17orf37 by gene-specific siRNA simultaneously reduced the DNA-binding activity of NF-κB, indicating C17orf37-mediated signaling may modulate *MMP-9*, *uPA* and *VEGF* genes through NF-κB pathway. This also justifies C17orf37 as an upstream signaling molecule of NF-κB. PI3K-Akt and mitogen-activated protein kinase are the two upstream signaling pathways that have been shown to be responsible for constitutive activation of IKK complex and NF-κB (Suh and Rabson, 2004). In prostate cancer cells, PI3K-Akt works like a signaling hub mainly as a downstream effector of tyrosine kinase growth factor receptors. Modulation of C17orf37 dramatically altered the phosphorylation of Akt at Ser-473 (Figure 6), which indicates C17orf37 may act as an inducer of Akt phosphorylation. The ratio of phosphorylated ERK1/2 to the total ERK1/2 also decreased, albeit minimally, when compared to the control-siRNA-treated DU-145 cells. This decrease in ERK1/2 phosphorylation may be due to the reduced expression of uPA protein upon C17orf37 silencing. In prostate cancer cells, uPA binds to its cell-surface receptor uPA-R thereby activating ERK1/2 signaling (Jo *et al*., 2005). Several studies have shown that knockdown of uPA abolishes the ERK1/2 phosphorylation (Aguirre Ghiso *et al*., 1999), indicating decrease in ERK1/2 phosphorylation in C17orf37 knockdown cells may be due to the downstream target molecule uPA.

Thus, based on our data, we propose a mechanistic model for C17orf37-mediated signaling in prostate cancer invasion and signaling (Figure 6d). In response to extracellular stimuli, growth receptors (tyrosine kinase) present on the prostate cancer cells cascade down the signal activating PI3K. This results in the activation of AKT that translocates to the membrane where it is phosphorylated at Ser-473 (Chan *et al*., 1999). Prenylated protein C17orf37 also remains localized to the cytosolic face of the membrane (may be as an adapter protein) and in turn controls the downstream signaling of activated p-AKT. Whether this effect is direct or mediated through other adapter proteins that physically interact with C17orf37 on the membrane

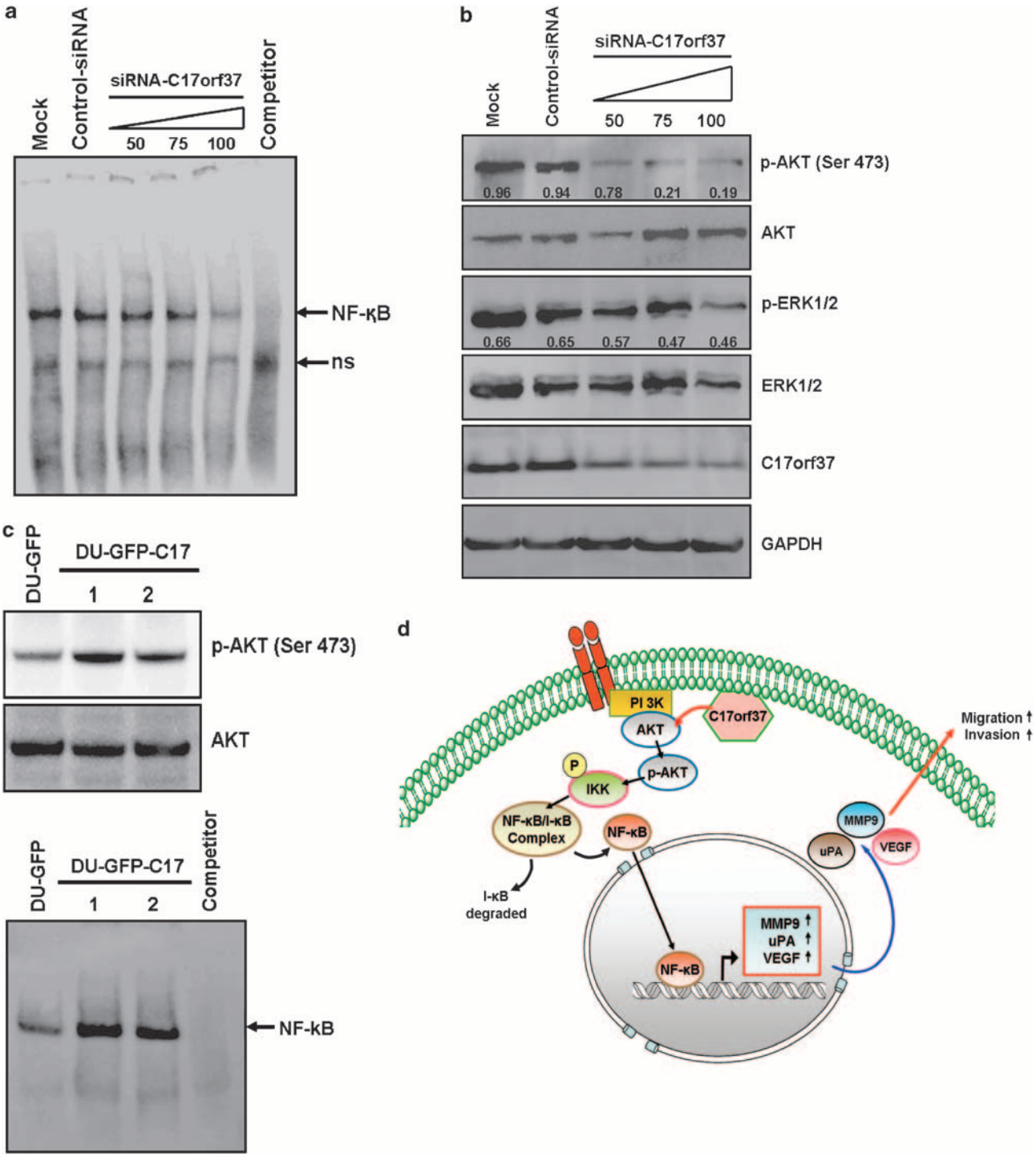

Figure 6 Knockdown of C17orf37 by siRNA reduces the nuclear factor-κB (NF-κB) DNA-binding activity by suppressing the AKT activation. (**a**) Electrophoretic mobility shift assay (EMSA) was carried out by incubating 5 μg of nuclear protein extracts from DU-145 cells treated with nontargeting siRNA (control siRNA) and 50, 75 and 100 nM siRNA specific to C17orf37. DU-145 cells treated with transfection media (mock) and in presence of competitive oligonucleotides to the probe (competitor) were used as controls. The nonsignificant band (NS) present in all the lanes did not have any effect even in the presence of competitor. (**b**) DU-145 prostate cancer cells were transiently transfected with nontargeting siRNA (control siRNA), and increasing concentration of C17orf37-specific siRNA at 50, 75 and 100 nM dose for 48 h. The expression of C17orf37, phospho-AKT (Ser 473), total AKT, phospho-ERK1/2 and total ERK1/2 was detected by western immunoblotting. Housekeeping gene glyceraldehyde-3-phosphate dehydrogenase (*GAPDH*) was used as loading control to normalize the total AKT and ERK1/2 protein levels, and then used to determine the ratio of the phosphorylated/total AKT and ERK, respectively. Numbers indicate the normalized expression ratio expressed as mean of three independent experiments. (**c**) Western immunoblotting showing phospho-AKT and total AKT (top panel), and EMSA showing NF-κB DNA-binding activity (bottom panel) in polyclonal populations overexpressing either DU-GFP (DU-145 stably expressing GFP vector) or DU-GFP-C17 (DU-145 stably expressing GFP-C17orf37) in two independent pools 1 and 2. Western blot and EMSA images are representative of three independent experiments. (**d**) Proposed working model for C17orf37 signaling in prostate cancer cells.

needs further investigation. Activated AKT phosphorylates IKK complex that then results in the translocation of NF-κB to the nucleus by reducing the half-life of IκBα (Suh and Rabson, 2004). In the nucleus NF-κB acts as transcription factor resulting in the enhanced expression of downstream target genes *MMP-9*, *uPA* and *VEGF*. These molecules are then secreted by prostate cancer cells and thereby increase the invasiveness of prostate cancer cells (Sliva, 2004).

In summary, we find that C17orf37 is highly expressed in prostate cancer cells and tissues, compared to minimal expression in normal prostate cells. C17orf37 is predominantly expressed as a membrane-bound cytosolic protein and actively regulates prostate cancer cell migration and invasion by upregulating the expression of MMP-9, uPA and VEGF. In addition, downregulation of C17orf37 by specific siRNA reduced the DNA-binding activity of NF-κB, substantiating the fact that C17orf37 expression contributes to the development of invasive prostate cancer through NF-κB-mediated downstream target genes. Interestingly, AKT activity was reduced due to *C17orf37* gene silencing suggesting membrane-bound C17orf37 may be a potential regulator of AKT phosphorylation. We believe our results are the first report to deduce the functional importance of so-called 'hypothetical protein' C17orf37 that may be considered as a potential therapeutic target for cancer therapy.

Materials and methods

Cell lines and culture conditions
Details describing cell culture and reagents are provided in the Supplementary information.

Cloning, expression and purification of recombinant C17orf37
Information about the plasmids constructed for the study and details about the protein expression and purification are given in Supplementary information.

Transfection procedures and siRNA-mediated gene silencing of C17orf37
Stable and transient transfection of DU-145, LNCaP and HPV18 C-1 cells was performed using Lipofectamine 2000 (Invitrogen, Carlsbad, CA, USA) with plasmid DNA (green fluorescent protein (GFP) vector or GFP-C17orf37). For C17orf37 knockdown experiments, human C17orf37 (NM_032339) smart pool siRNA (siRNA-C17orf37) and human nontargeting scrambled siRNA duplex (control siRNA) were purchased from Dharmacon (Lafayette, CO, USA) and transfected in DU-145 cells according to manufacturer's instructions. Details are provided in Supplementary information.

Isolation of total RNA and quantitative reverse-transcription PCR
Information about the RNA extraction and q-RT–PCR is included in Supplementary information.

Cell fractionation and immunoblotting
Whole-cell protein extracts were prepared from prostate cell lines as described previously (Das *et al*., 2007). Cytosolic and nuclear fractions of DU-145 and LNCaP cells were prepared using the NE-PER nuclear and cytoplasmic extraction kit (Pierce, Rockford, IL, USA) according to the manufacturer's instructions. Bacterial cell lysates were prepared using B-PER extraction kit (Pierce). Western immunoblot was performed using a 15% gel for C17orf37 protein analysis and 10% for other proteins, as described previously (Das *et al*., 2007). List of antibodies purchased for the study is included in the Supplementary information.

Mass spectrometry and liquid chromatography–tandem mass spectrometry
Mass spectrometry was performed using FTICR instrument (LTQ-FT; Thermo Fisher, San Jose, CA, USA) as described in Supplementary information.

Confocal microscopy, immunofluorescence and TIRFM
DU-145 and LNCaP cells were grown on glass coverslips and treated with C17orf37 antibody (Zymed, Carlsbad, CA, USA). For confocal images, cells were visualized on a Zeiss LSM 410 confocal microscope and images were captured using LSM 4 software (Carl Zeiss Microimaging). For, TIRFM, cells were grown on coverslips and then fixed by 2% paraformaldehyde. Unpermeabilized cells were then washed with PBS and treated with C17orf37 or tubulin antibody (Calbiochem) followed by Alexa-568-conjugated secondary antibody. Coverslips were then mounted on specialized cover glass 1 (22×50 mm size; Corning, Lowell, MA, USA). For TIRF images, cells were visualized on an Olympus IX71 microscope with commercial TIRF attachment as described previously (Burghardt *et al*., 2006) by $\times 60$ oil immersion objective.

Immunohistochemistry
Frozen prostate tumors from patients were provided by the UNMC/Eppley Cancer Center Tumor Bank (Omaha, NE, USA). Two anatomic pathologists independently graded the H&E-stained sections and Gleason scores for these tissues varied between 6 and 10. Immunohistochemistry was performed as described previously (Das *et al*., 2007). C17orf37 antibody (Zymed) and rabbit IgG (Sigma, St Louis, MO, USA) were used for the immunohistochemistry study. Representative images of the clinical prostate sections were captured and analysed by the pathologist.

Cell migration assays
At 48-h after transfection with siRNA-C17orf37 or control siRNA, 1×10^6 number of DU-145 cells were mixed with low melting agarose and growth medium to form a semisolid gel and migration assay was performed as described before (Das *et al*., 2007). The cells were allowed to migrate out of the semisolid beads for 36 h and then visualized on an Olympus microscope (Carl Zeiss). Representative images of the cells were captured and the number of cells that migrate out of the beads was counted from three independent experiments. Fold change of migration was determined by a ratio of migrated cells in experimental group to the control group.

In vitro *tumor invasion assay*
Tumor invasion assay was performed using BD Biocoat Tumor Invasion System (BD Biosciences, Bedford, MA, USA) according to the manufacturer's instructions. Details about the procedure are given in Supplementary information.

Reverse transcription–PCR
One-step RT–PCR (Invitrogen) was performed using 1 μg of total RNA as described before (Das *et al*., 2007). Custom primers were synthesized as mentioned in Supplementary Table 1.

ELISA assay for MMP-9 and VEGF
ELISA assay performed from the conditioned media as described in Supplementary Materials and methods section.

Electrophoretic mobility shift assay
NF-κB DNA-binding activity was determined by gel-shift assay in C17orf37 knockdown and overexpressed cells using NF-κB-specific EMSA gel-shift assay kit (Panomics Inc., Redwood, CA, USA).

Statistical analyses
Results were expressed as mean and statistical analysis performed using GraphPad Prism 4.02 software (San Diego, CA, USA). One sample *t*-test was performed and $P<0.05$ was considered to be significant.

Conflict of interest

Research projects of Drs Vishwanatha, Prokai and Borejdo are supported by funds from the National Institutes of Health. The authors declare no other conflict of interest.

Acknowledgements

We thank Dr Linda Cunnighum (UNTHSC) for assistance with immunohistochemistry and Dr Kapil Mehta (MD Anderson Cancer Center, TX) for help with migration assays. The present work is supported by grant nos. CA109593 and MD 001633 (JKV) from NIH and DOD PCRP Training Award PC081282 (SD). UNMC/Eppley Cancer Center Tumor Bank was supported by an NCI Cancer Center Support Grant P30 CA36727 and Nebraska Department of Health Institutional LB595 Grant for Cancer and Smoking Disease Research.

References

Aguirre Ghiso JA, Kovalski K, Ossowski L. (1999). Tumor dormancy induced by downregulation of urokinase receptor in human carcinoma involves integrin and MAPK signaling. *J Cell Biol* **147**: 89–104.

Arya M, Bott SR, Shergill IS, Ahmed HU, Williamson M, Patel HR. (2006). The metastatic cascade in prostate cancer. *Surg Oncol* **15**: 117–128.

Axelrod D. (2001). Selective imaging of surface fluorescence with very high aperture microscope objectives. *J Biomed Opt* **6**: 6–13.

Banerjee AG, Liu J, Yuan Y, Gopalakrishnan VK, Johansson SL, Dinda AK *et al*. (2003). Expression of biomarkers modulating prostate cancer angiogenesis: differential expression of annexin II in prostate carcinomas from India and USA. *Mol Cancer* **8**: 2–34.

Berger R, Lin DI, Nieto M, Sicinska E, Garraway LA, Adams H *et al*. (2006). Androgen-dependent regulation of her-2/neu in prostate cancer cells. *Cancer Res* **66**: 5723–5728.

Burghardt TP, Ajtai K, Borejdo J. (2006). *In situ* single-molecule imaging with attoliter detection using objective total internal reflection confocal microscopy. *Biochemistry* **45**: 4058.

Chan TO, Rittenhouse SE, Tsichlis PN. (1999). AKT/PKB and other D3 phosphoinositide-regulated kinases: kinase activation by phosphoinositide-dependent phosphorylation. *Annu Rev Biochem* **68**: 965–1014.

Connolly JM, Rose DP. (1998). Angiogenesis in two human prostate cancer cell lines with differing metastatic potential when growing as solid tumors in nude mice. *J Urol* **160**: 932–936.

Das S, Roth CP, Wasson LM, Vishwanatha JK. (2007). Signal transducer and activator of transcription-6 (STAT6) is a constitutively expressed survival factor in human prostate cancer. *Prostate* **67**: 1550–1564.

Eeles RA, Kote-Jarai Z, Giles GG, Olama AA, Guy M, Jugurnauth SK *et al*. (2008). Multiple newly identified loci associated with prostate cancer susceptibility. *Nat Genet* **40**: 316 .

Evans EE, Henn AD, Jonason A, Paris MJ, Schiffhauer LM, Borrello MA *et al*. (2006). C35 (C17orf37) is a novel tumor biomarker abundantly expressed in breast cancer. *Mol Cancer Ther* **5**: 2919.

Fresno Vara JA, Casado E, de Castro J, Cejas P, Belda-Iniesta C, Gonzalez-Baron M. (2004). PI3K/Akt signalling pathway and cancer. *Cancer Treat Rev* **30**: 193–204.

Fu HW, Casey PJ. (1999). Enzymology and biology of CaaX protein prenylation. *Recent Prog Horm Res* **54**: 315.

Helenius MA, Savinainen KJ, Bova GS, Visakorpi T. (2006). Amplification of the urokinase gene and the sensitivity of prostate cancer cells to urokinase inhibitors. *BJU Int* **97**: 404–409.

Hicklin DJ, Ellis LM. (2005). Role of the vascular endothelial growth factor pathway in tumor growth and angiogenesis. *J Clin Oncol* **23**: 1011–1027.

Huang S, Pettaway CA, Uehara H, Bucana CD, Fidler IJ. (2001). Blockade of NF-kappaB activity in human prostate cancer cells is associated with suppression of angiogenesis, invasion, and metastasis. *Oncogene* **20**: 4188–4197.

Jo M, Thomas KS, Marozkina N, Amin TJ, Silva CM, Parsons SJ *et al*. (2005). Dynamic assembly of the urokinase-type plasminogen activator signaling receptor complex determines the mitogenic activity of urokinase-type plasminogen activator. *J Biol Chem* **280**: 17449–17457.

Kauraniemi P, Kallioniemi A. (2006). Activation of multiple cancer-associated genes at the ERBB2 amplicon in breast cancer. *Endocr Relat Cancer* **13**: 39.

Kelly P, Stemmle LN, Madden JF, Fields TA, Daaka Y, Casey PJ. (2006). A role for the G12 family of heterotrimeric G proteins in prostate cancer invasion. *J Biol Chem* **281**: 26483–26490.

Li Y, Cozzi PJ. (2007). Targeting uPA/uPAR in prostate cancer. *Cancer Treat Rev* **33**: 521–527.

Lokeshwar BL. (1999). MMP inhibition in prostate cancer. *Ann NY Acad Sci* **878**: 271–289.

Maurer-Stroh S, Eisenhaber F. (2005). Refinement and prediction of protein prenylation motifs. *Genome Biol* **6**: R55.

Myers RB, Srivastava S, Oelschlager DK, Grizzle WE. (1994). Expression of p160erbB-3 and p185erbB-2 in prostatic intraepithelial neoplasia and prostatic adenocarcinoma. *J Natl Cancer Inst* **86**: 1140–1145.

Pienta KJ, Loberg R. (2005). The 'emigration, migration, and immigration' of prostate cancer. *Clin Prostate Cancer* **4**: 24–30.

Price JT, Bonovich MT, Kohn EC. (1997). The biochemistry of cancer dissemination. *Crit Rev Biochem Mol Biol* **32**: 175.

Rothermund CA, Kondrikov D, Lin MF, Vishwanatha JK. (2002). Regulation of bcl-2 during androgen-unresponsive progression of prostate cancer. *Prostate Cancer Prostatic Dis* **5**: 236.

Sheng S. (2001). The urokinase-type plasminogen activator system in prostate cancer metastasis. *Cancer Metastasis Rev* **20**: 287–296.

Sliva D. (2004). Signaling pathways responsible for cancer cell invasion as targets for cancer therapy. *Curr Cancer Drug Targets* **4**: 327.

Suh J, Rabson AB. (2004). NF-kappaB activation in human prostate cancer: important mediator or epiphenomenon? *J Cell Biochem* **91**: 100–117.

Sun J, Zheng SL, Wiklund F, Isaacs SD, Purcell LD, Gao Z *et al*. (2008). Evidence for two independent prostate cancer risk-associated loci in the *HNF1B* gene at 17q12. *Nat Genet* **40**: 1153–1155 .

Thalmann GN, Anezinis PE, Chang SM, Zhau HE, Kim EE, Hopwood VL *et al*. (1994). Androgen-independent cancer progression and bone metastasis in the LNCaP model of human prostate cancer. *Cancer Res* **54**: 2577.

Virtanen SS, Vaananen HK, Harkonen PL, Lakkakorpi PT. (2002). Alendronate inhibits invasion of PC-3 prostate cancer cells by affecting the mevalonate pathway. *Cancer Res* **62**: 2708–2714.

Wilson MJ, Sinha AA. (1993). Plasminogen activator and metalloprotease activities of Du-145, PC-3, and 1-LN-PC-3-1A human prostate tumors grown in nude mice: correlation with tumor invasive behavior. *Cell Mol Biol Res* **39**: 751–760.

Wilson SR, Gallagher S, Warpeha K, Hawthorne SJ. (2004). Amplification of MMP-2 and MMP-9 production by prostate cancer cell lines via activation of protease-activated receptors. *Prostate* **60**: 168–174.

Winter-Vann AM, Casey PJ. (2005). Post-prenylation-processing enzymes as new targets in oncogenesis. *Nat Rev Cancer* **5**: 405–412.

Woolard J, Wang WY, Bevan HS, Qiu Y, Morbidelli L, Pritchard-Jones RO *et al*. (2004). VEGF165b, an inhibitory vascular endothelial growth factor splice variant: mechanism of action, *in vivo* effect on angiogenesis and endogenous protein expression. *Cancer Res* **64**: 7822–7835.

Wu HC, Hsieh JT, Gleave ME, Brown NM, Pathak S, Chung LW. (1994). Derivation of androgen-independent human LNCaP prostatic cancer cell sublines: role of bone stromal cells. *Int J Cancer* **57**: 406–412.

Supplementary Information accompanies the paper on the Oncogene website (http://www.nature.com/onc)

Supplementary Table 1 *Primer Sequences*

Gene	**Sequence (5′-3′)**	**Amplified Size(bp)**
C17orf37 Forward	CAGTGCTGTGAAGGAGCAGT	202
C17orf37 Reverse	GACGGCTGTTGGTGATCTTT	
VEGF Forward (Munaut *et al.*, 2003)	CCTGGTGGACATCTTCCAGGAGTA	407 -$VEGF_{165}$ 275 -$VEGF_{121}$
VEGF Reverse	CTCACCGCCTCGGCTTGTCACA	
MMP-9 Forward	TTGACAGCGACAAGAAGTGG	185
MMP-9 Reverse	GCCATTCACGTCGTCCTTAT	
uPA Forward	TTGACAGCGACAAGAAGTGG	781
uPA Reverse	CTACAGCGCTGACACGCTTG	
β-actin Forward	GAGGCTCTCTTCCAGCCTTCCTTCCT	308
β-actin Reverse	CCTGCTTGCTGATCCACATCTGCTGG	

Supplementary Table 2 *SMART Pool Duplex for C17orf37 (Dharmacon)* Sequences were BLAST searched in NCBI database to determine the specificity with C17orf37 sequence. All the sequences were confirmed to be 100 percent homology with only C17orf37 sequence.

1	Sense Sequence	C.C.G.A.A.G.A.G.C.C.A.G.U.A.A.U.G.G.A.U.U
	Antisense Sequence	5′-p.U.C.C.A.U.U.A.C.U.G.G.C.U.C.U.U.C.G.G.U.U
2	Sense Sequence	U.A.A.A.U.G.G.A.C.A.G.C.U.G.G.U.G.U.U.U.U
	Antisense Sequence	5′-p.A.A.C.A.C.C.A.G.C.U.G.U.C.C.A.U.U.U.A.U.U
3	Sense Sequence	U.A.G.A.A.A.A.G.A.U.C.A.C.C.A.A.C.A.G.U.U
	Antisense Sequence	5′-p.C.U.G.U.U.G.G.U.G.A.U.C.U.U.U.U.C.U.A.U.U
4	Sense Sequence	G.G.A.G.C.A.G.U.A.U.C.C.G.G.G.C.A.U.C.U.U
	Antisense Sequence	5′-p.G.A.U.G.C.C.C.G.G.A.U.A.C.U.G.C.U.C.C.U.U

Supplementary Methods

Cloning, expression and purification of recombinant C17orf37

Full length human C17orf37 cDNA of 347 bp was amplified using a forward primer 5′-CTAGAATTCCACATGAGCGGGGAGCC-3′ containing an Eco*R*I restriction site and a reverse primer 5′-AGACTCGAGTGCAGTCACAGGATGA-3′ containing a *XhoI* restriction site, and cloned into pGEX-4T-1 vector (GE Healthcare, Piscataway, NJ) in proper reading frame. GST-C17orf37 fused protein was expressed in E.coli Bl-21 strain and purified using Glutathione Sepharose 4B column (GE Healthcare, Piscataway, NJ) according to manufacturer's instructions. Purified GST-C17orf37 was cleaved with 20 units/mg thrombin enzyme (Sigma, St.Louis, MO) overnight at room temperature to remove the GST tag. Recombinant C17orf37 is finally eluted from HiTrap Benzamidine FF columns (GE Healthcare, Piscataway, NJ) to remove the residual thrombin enzyme.

Full length human C17orf37 cDNA of 347bp was amplified using a forward primer 5′-CAAGCTTCGAATTCAATGAGCGGG-3′ containing an *EcoR*I restriction site and a reverse primer 5′-ATCCGGTGGATCCAGTCACAG-3′ containing a *BamH*I restriction site. PCR products were cloned into the pEGFP-C1 vector and the resulting vector was named GFP-C17orf37.

Cell lines and culture conditions

DU-145, PC-3, LNCaP C4-2, LNCaP-R, RF and UR prostate cancer cells were maintained in RPMI1640 supplemented with 10% fetal bovine serum (FBS) and

1% penicillin-streptomycin (PS). Prostate epithelial cell lines HPV18 C-1 and PWR-1E were maintained in keratinocyte-SFM (Invitrogen, Carlsbad, CA) supplemented with bovine pituitary extract (25µg/ml) and recombinant epidermal growth factor (0.15ng/ml).

Mass spectrometry and liquid chromatography–tandem mass spectrometry

A hybrid linear ion trap–Fourier transform ion cyclotron resonance (7-Tesla) instrument (LTQ-FT, Thermo Fisher, San Jose, CA) equipped with an electrospray ionization (ESI) source and operated with the Xcalibur (version 2.2) data acquisition software was used for all mass spectrometric (MS) analyses (Branca *et al.*, 2007).

The molecular weight of the recombinant protein was determined by direct infusion (protein solution in aqueous solution containing 50% methanol and 1% acetic acid) using FTICR prior to reduction and carbamidomethylation of cysteines. Mass resolution (M/ΔM) was set to 200,000 at *m/z* 400 and defined as full width at half maximum (FWHM) of the peak.

About 20-fold excess of dithiothreitol (in mass) was added to reduce the protein at 50 ºC for 20 min, followed by alkylation with iodoacetamide (about 50:1 weight ratio iodoacetamide to protein) at room temperature for 30 min in the dark. The resulting carbamidomethylated protein solution was then desalted by repeated centrifugation in microcon filters (Millipore, Billerica, MA) at 8000*g*. Typtic peptides were obtained by incubation of the protein with trypsin (Promega,

Madison, WI; ~50:1 protein to trypsin molar ratio) for 24 h at 37 ºC in 50 mM ammonium bicarbonate (pH 7.8).

For online RP-HPLC-tandem mass spectrometric analysis of the tryptic digest (Stevens *et al.*, 2008), 5 µl of the sample was loaded onto a PepMap C18 capillary trap (LCPackings, Sunnyvale, CA) and desalted with 3% acetonitrile, 1% acetic acid for 5 min prior to injection onto a 75 µm i.d. x 10 cm PicoFrit C18 analytical column (New Objective, Woburn, MA). Following peptide desalting and injection onto the analytical column, a linear gradient provided by a Surveyor MS pump (Thermo) was carried out to 40% acetonitrile in 60 min at 250 nL/min. Spray voltage and capillary temperature during the gradient run were maintained at 2.0 kV and 250 °C, respectively. The conventional data-dependent mode of acquisition was utilized in which an accurate *m/z* survey scan was performed in the FTICR cell followed by parallel recording of tandem mass spectra (MS/MS) in the linear ion trap of the top 10 most intense precursor ions. FTICR full-scan mass spectra were acquired at 100,000 mass resolving power (m/z 400) from m/z 350 to 1500 using the automatic gain control mode of ion trapping (500000 target ion count). Collision-induced dissociation (CID) was performed in the linear ion trap using a 2.0-u isolation width and 35% normalized collision energy with helium as the target gas.

MS/MS data generated by data dependent acquisition via the LTQ-FT were extracted by the manufacturer's BioWorks version 3.3 software and searched against a composite IPI human protein database containing both forward and randomized sequences using the Mascot (version 2.2.1; Matrix

Science, Boston, MA) search algorithm. Mascot was searched with a fragment ion mass tolerance of 0.80 Da and a parent ion tolerance of 10 ppm assuming the digestion enzyme trypsin with the possibility of one missed cleavage. Carbamidomethylation of cysteine was specified as a static modification, while oxidation of methionine, conversion of N-terminal Glu/Gln (E/Q) to pyroglutamyl (<E) in tryptic peptides and N-terminal protein acetylation were specified as variable modifications in the database search. The software program Scaffold (version Scaffold-01_06_13, Proteome Software Inc., Portland, OR) was then employed to compile and validate tandem MS-based peptide and protein identifications. Peptide identifications were accepted at greater than 95.0% probability as determined by the Peptide Prophet algorithm (Keller *et al.*, 2002).

Isolation of total RNA and quantitative reverse transcription-PCR

Total RNA was isolated from prostate cells by Trizol reagent (Invitrogen, Carlsbad, CA) according to manufacturer's instructions. For quantitative reverse transcription-PCR (qRT-PCR) analysis, a two step process was performed using the SuperScript III platinum Two-step qRT-PCR kit with SYBR Green (Invitrogen, Carlsbad, CA). One μg of isolated RNA was used for conversion to cDNA followed by amplification using a Cepheid Smart Cycler system (Cepheid, Sunnyvale, CA). Ct values were determined at a threshold value of 30 fluorescence units. Samples were run in triplicate and housekeeping gene actin was used as an internal control. The fold change of C17orf37 mRNA expression was calculated according to the formula of Livak and Schmittgen (Livak and

Schmittgen, 2001) with respect to HPV18 C-1 cell line which was fixed to base line as 1.

Transfection procedures

Cells were grown to 85-90% confluency and transfected with plasmid DNA (GFP-C17orf37 vector or empty vector-GFP) for a period of 6 hours in OPTI-MEM (Invitrogen, Carlsbad, CA). After transfections, cells were grown in complete media overnight before mounting on slides using Vectashield (Vector Laboratories, Burlingame, CA) for confocal microscopy.

For generation of stable cells (DU-GFP and DU-ORF cells), stably transfected cell populations were selected in RPMI supplemented with 10% FBS and 500µg/ml G418 (Invitrogen, Carlsbad, CA) for about 1 month. Selected colonies (3-5) were then separately cultured to obtain the subclones (ORF#9 and ORF#11 for GFP-C17orf37 plasmid and GFP#1 for GFP plasmid (vector control) in DU-145 cells). Stable cells were then characterized by western immunoblotting and confocal microscopy.

Smart pool siRNA sequences for C17orf37 are listed in Supplementary Table 2.

ELISA assay for MMP-9 and VEGF

DU-145 cells were seeded in 6 well plates and transiently transfected with mock (Dharmafect), non-targeting control siRNA and C17orf37 siRNA; and lipofectamine (mock), GFP vector only, GFP-C17orf37 as mentioned in the transfection procedure section in the Material and methods. After transfections,

cells were incubated in serum free RPMI (Invitrogen) for 24 hours. The culture medium was collected, centrifuged to remove cell debris and stored at -80°C until assay. The number of cells per well was counted using hemocytometer. Quantikine Human MMP-9 and VEGF Elisa assay kit (R & D Systems, Minneapolis, MN) was used to determine the concentration of secreted MMP-9 and VEGF, according to the manufacturer's instructions. MMP-9 concentration (ng/mL) was calculated and normalized to the number of cells (ng/mL/10^5 cells). Quantikine VEGF elisa kit determines both $VEGF_{121}$ and $VEGF_{165}$ secreted isoform concentration (pg/mL) and normalized to the total number of cells (pg/mL/10^5 cells). The concentration values are graphically represented as ratio of control to the untreated cells.

Antibodies

Antibodies used for the study are as follows: C17orf37 (Abnova, Taiwan; 1:500) and C17orf37 (anti-C35) (Zymed, Carlsbad, CA); Glyceraldehyde 3-phosphate dehydrogenase (GAPDH) (Santa Cruz Biotechnology, Santa Cruz, CA, 1:1250 dilution); actin (Calbiochem, San Diego, CA; 1:2000 dilution); Lamin (1:1000), MMP-9 (1:1000), Akt (1: 1000) and phospho-Akt Ser-473 (1:500) dilutions from Cell Signaling, Danvers, MA; uPA (1:500) and VEGF (1:250) dilutions from R & D Systems, Minneapolis, MN; and ERK1/2 (1:1000) and phospho-ERK1/2 Thr-202/Tyr-204 (1:500) dilutions BD Biosciences, San Jose, CA.

In vitro Tumor Invasion Assay

Transiently transfected DU-145 cells with either GFP-vector or GFP-C17orf37; siRNA-C17orf37 or control-siRNA (as described before), and stable DU-GFP, DU-ORF-9 and DU-ORF-11 cell suspensions were prepared in growth medium without serum and $2.5x10^4$ cells/well were added to the top chamber of the tumor invasion system and 10% FBS was added to the bottom chambers as chemoattractant. Cells were allowed to invade through the Matrigel for 24 hours at 37°C. Following incubation, nonmigratory cells were removed from the top chamber and the cells that successfully invade the Matrigel matrix and migrate to the bottom side of the membrane were stained with 4µg/ml of Calcein AM (Molecular Probes, Carlsbad, CA) and fluorescent reading was taken at excitation/emission wavelengths of 485/530 nm. Growth medium incubated without any cells in the invasion system was used as blank reading and three independent experimental readings were used to calculate the mean fold change of invasion by determining the ratio of fluorescent reading-experimental group to fluorescence reading-control group.

Electrophoretic Mobility Shift Assay (EMSA)

Cells were treated with siRNA-C17orf37 at 50, 75 and 100 nM concentrations or control-siRNA as described before. Nuclear extract was prepared using NE-PER cytosolic nuclear extraction kit (Pierce, Rockford, IL). 5 µg of nuclear protein

extracts was used to incubate with the biotin conjugated probe according to manufacturer's instructions.

Scratch Wound Healing Migrating Assay

DU-ORF-9 cells were grown on coverslip in a monolayer and scratch was created using pipet tip. Floating cells were removed by changing the medium and cells were imaged at different time points 0, 3, 6 and 9 hours after the creating of the wound. Cells were then washed, fixed, permeabilized and imaged using confocal microscopy.

Supplementary Figure Legends

Supplementary Figure 1 Expression of C17orf37 in prostate cancer cells. Total RNA was isolated from DU-145, PC-3, LNCaP-R and HPV-18 C-1. *C17orf37* gene was amplified by RT-PCR as described in materials and methods section. GST-C17orf37 vector (as described in Materials and Methods section) was used as positive control. *β-Actin* was used as loading control. C17orf37 mRNA was found to be highly expressed in DU-145, PC-3 and LNCaP-R prostate cancer cells compared to minimal expression in HPV-18C1 prostate epithelial cells.

Supplementary Figure 2 Mass spectrum of recombinant C17orf37 protein. Full-scan FTICR mass spectrum acquired of the purified recombinant protein at 200,000 mass resolving power at m/z 400. The resolving power obtained for the +9 charge state isotope cluster ($[M+9H]^{9+}$, inset) was ~ 55,000 (FWHM).

Supplementary Figure 3 Overexpression of C17orf37 increases invasive potential of DU-145 cells. Stable cells DU-GFP, DU-ORF-9 and DU-ORF11, and parental DU-145 cells were seeded onto matrigel coated tumor invasion chambers and allowed to migrate toward serum for 24 hours at 37°C. Fold change of invasion was calculated as described in supplementary materials and methods section. *Columns* are mean of three independent experiments; *bars*, SD. **, $P < 0.001$, relative to DU-GFP cells; statistical analysis included Student's *t* test for calculating significant differences within groups.

Supplementary Figure 4 Graphical representation showing expression ratio of p-Akt/Akt and p-ERK/ERK normalized to housekeeping gene GAPDH as shown in Figure 6b. *Columns* mean of four independent experiments; *bars*, SD. **, *P* <0.005 relative to mock treated.

Supplementary Figure 5 Confocal microscopy showing the expression of C17orf37 preferentially localized to the leading edge of the migrating DU-ORF-9 cells. Cells were grown on coverslip in a monolayer and scratch was created as described in the Supplementary information. After 3 hours, cells were fixed in a slide and imaged using LSM510 confocal microscopy (phase contrast and fluorescence at 488 nm wavelength). Inset shows the magnified image of the area marked with dotted box. Dotted arrow at the top indicates the direction of migration and solid arrows indicate the migrating cells with protruding edge. Original magnification, *X100*.

References

Branca RM, Bodo G, Bagyinka C, Prokai L. (2007). De novo sequencing of a 21-kDa cytochrome c4 from thiocapsa roseopersicina by nanoelectrospray ionization ion-trap and fourier-transform ion-cyclotron resonance mass spectrometry. *J. Mass Spectrom.* **42:**1569-1582.

Keller A, Nesvizhskii AI, Kolker E, Aebersold R. (2002). Empirical statistical model to estimate the accuracy of peptide identifications made by MS/MS and database search. *Anal. Chem.* **74:**5383-5392.

Livak KJ, Schmittgen TD. (2001). Analysis of relative gene expression data using real-time quantitative PCR and the 2(-delta delta C(T)) method. *Methods* **25:**402-408.

Munaut C, Noel A, Hougrand O, Foidart JM, Boniver J, Deprez M. (2003). Vascular endothelial growth factor expression correlates with matrix metalloproteinases MT1-MMP, MMP-2 and MMP-9 in human glioblastomas. *Int. J. Cancer* **106:**848-855.

Stevens SM,Jr, Duncan RS, Koulen P, Prokai L. (2008). Proteomic analysis of mouse brain microsomes: Identification and bioinformatic characterization of

endoplasmic reticulum proteins in the mammalian central nervous system. *J. Proteome Res.*

Supplementary Figure 1

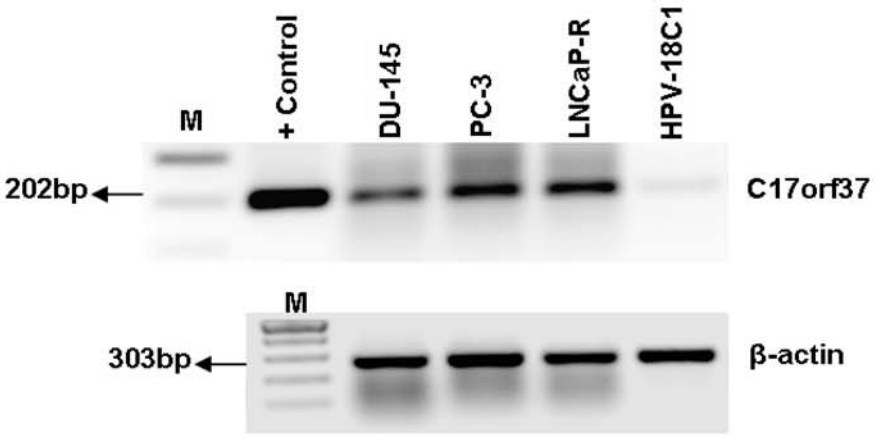

Supplementary Figure 2

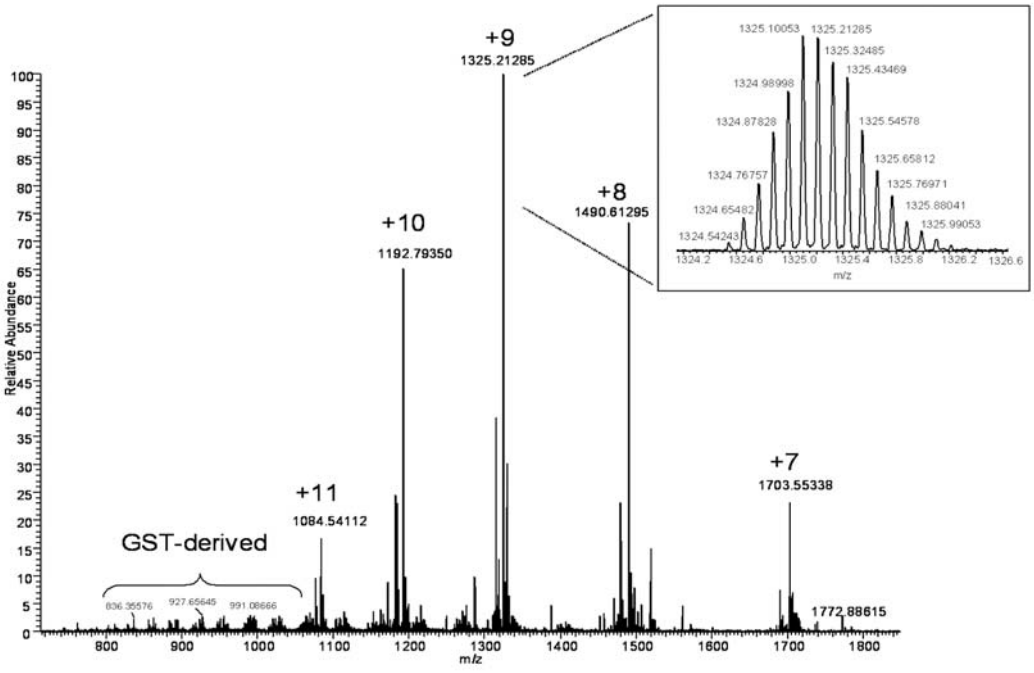

Supplementary Figure 3

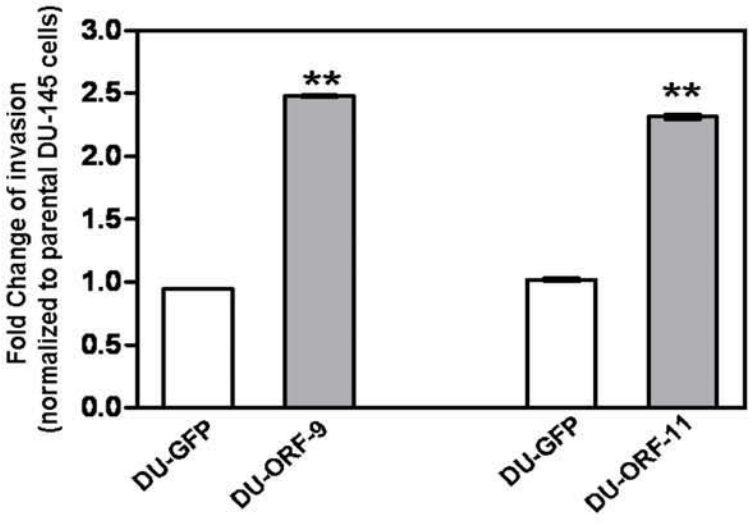

Supplementary Figure 4

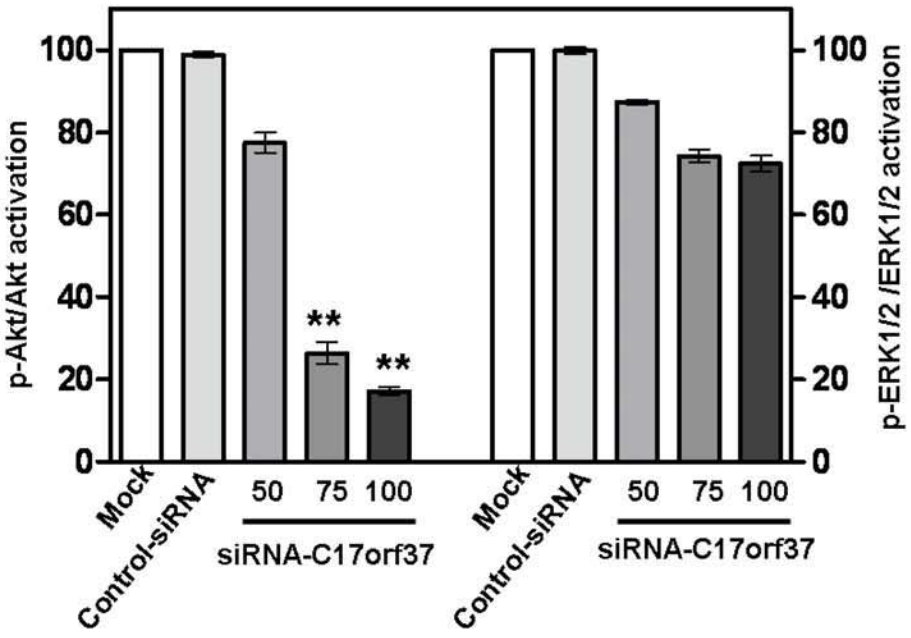

Supplementary Figure 5

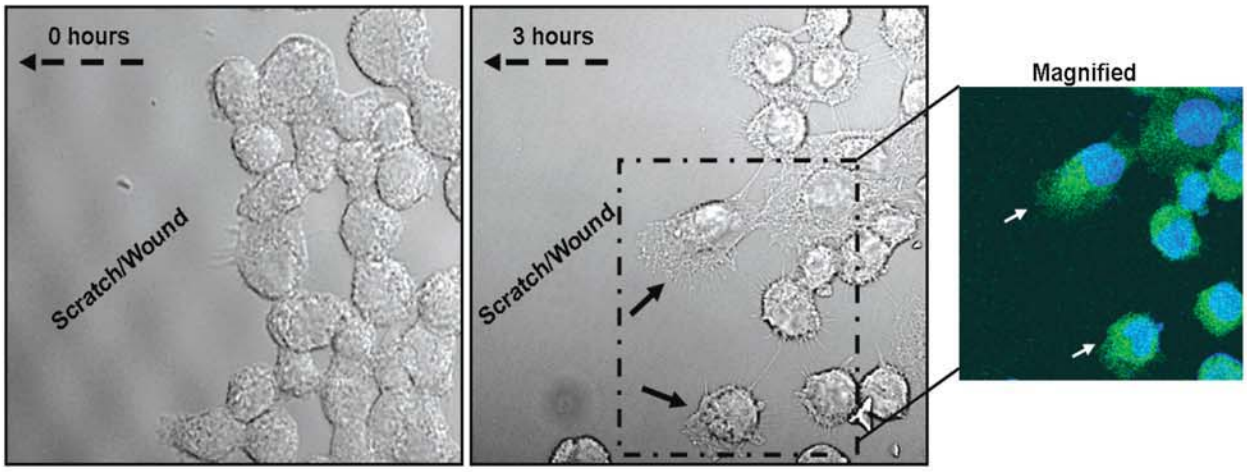

Abstract: A9

Importance of C17orf37 prenyl modification of C17orf37 in cancer cell migration and invasion

Subhamoy Dasgupta and Jamboor K Vishwanatha
Department of Biomedical Sciences and Institute for Cancer Research, University of North Texas Health Science Center, 3500 Camp Bowie Blvd, Fort Worth, TX, 76107

C17orf37 is a novel gene located in the hot spot locus of human chromosomal region 17q12-21. *C17orf37* is frequently amplified in breast cancer patients along with *ERBB2*, and expression correlates with grade and stage of cancer. *C17orf37* gene is also found to be activated in certain cancer cells and tissues irrespective of *ERBB2* status, compared to minimal expression in normal cells. Recently, we have reported that C17orf37 is highly overexpressed in prostate cancer cells and tissues, and expression of the gene positively correlates with the migratory and invasive potential of cancer cells. Moreover C17orf37 acts as a signaling molecule via Akt/NF-κB pathway modulating the expression of key metastasis-related genes uPA, MMP-9 and VEGF. We identified a putative prenylation motif 'CVIL' at the C-terminal end of C17orf37 protein. Using confocal, total internal reflection fluorescence microscopy (TIRFM) and cellular fractionation studies we show C17orf37 is post-translationally modified by GGTase-I enzyme, which translocates the protein to the inner leaflet of plasma membrane. Mutation of the cys-112 or entire deletion of the 'CVIL' motif of C17orf37 protein blocks the protein localization to the membrane. Based on this, we hypothesize that prenylation at 'CVIL' motif is important for activation of C17orf37 protein and subsequent downstream signaling. To study the importance of prenylated C17orf37 in cancer cells, we generated stable cells expressing either wild type or mutant C17orf37 protein. Our studies show that prenylated C17orf37 protein (wild type) preferentially localize to the leading edge of migrating cancer cells (directional) thereby activating nucleation of F-actin, formation of lamellipodia and increased migration of cancer cells. Cells expressing mutant C17orf37 protein are mostly localized in the cytosol and fail to localize to the edge of the migrating cancer cells. In addition, we identified a canonical immunoreceptor tyrosine-based activation motif (ITAM) at the N-terminus of C17orf37 protein. Currently we are investigating the importance of ITAM domain for downstream signaling of C17orf37 through Akt/NF-κB pathway.

(Supported by NIH grants CA109593 and MD 001633 to JKV and Department of Defense Predoctoral Training Award PC081282 to SD.)